Morphological and Cytochemical Studies of Fertilization in a Red Alga, *Palmaria palmata* O. Kuntze

Ichiro Mine

Institute of Algological Research
Facultly of Science
Hokkaido University

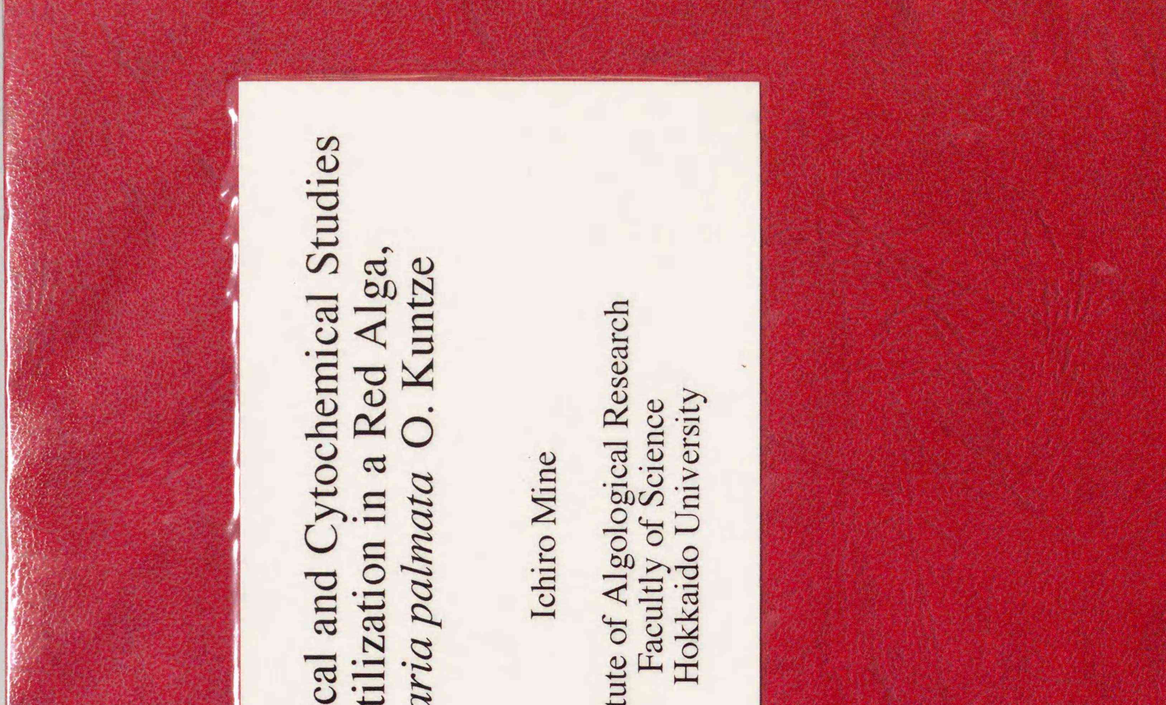

Morphological and Cytochemical Studies of Fertilization in a Red Alga, Palmaria palmata *O. Kuntze*

Morphological and cytochemical studies of fertilization in a red alga, *Palmaria palmata* O. Kuntze

by

Ichiro Mine

Institute of Algological Research,
Faculty of Science,
Hokkaido University

CONTENTS

ACKNOWLEDGEMENTS

I am very grateful to Professor Masakazu Tatewaki for his kind guidance and encouragement during the present studies. I would like to express thanks to Dr. Taizo Motomura for kind teaching of electron microscopic techniques and helpful suggestions.

Special thanks go to Dr. Christine A. Maggs, Queen's University, U.K., Dr. Lynda J. Goff, University of California, Dr. Annette W. Coleman, Brown University, U.S.A., and Dr. Terunobu Ichimura for their critical reading of the manuscript and improving the English usage.

I also appreciate Drs. Isamu Wakana and Geetangeli V. Deshmukhe giving friendly and practical advice. And I am thankful to various forms of help from Mr. Takashi Denboh, Mr. Hirofumi Aruga and staffs of the Institute of Algological Research.

INTRODUCTION

Fertilization in red algae is achieved by fusion between a non-flagellated spermatium, liberated from a male gametophyte, and a trichogyne, the specialized process of a carpogonium (egg cell) formed on a female gametophyte. The occurrence of amoeboid movement in red algal spermatia has frequently been noted (Dixon 1973), so it is difficult to exclude chemotactic processes in gamete recognition in red algae. However, it is probable that taxon- and organ-specific recognition and attachment between red algal gametes are principally governed by the adhesiveness of the cell surface structures of the gametes (Dixon 1973, Kim & Fritz 1993). Therefore, red algal gametes provide good material for studying specific cell-to-cell adhesion.

Several other physiological events are also indispensable for fertilization processes in red algae. Following successful attachment of a spermatium, localized cell wall breakdown of a trichogyne must occur before cytoplasmic fusion of the gametes. The male (or spermatium) nucleus that invades from the attached spermatial cell must migrate scores of micrometers inside the trichogyne toward the base of the carpogonium where it can fuse with the carpogonial nucleus. It has been reported in previous light microscopic studies (Grubb 1925, Fritsch 1945, p.596, Drew 1951, Magne 1952, Mumford & Cole 1977) as well as in TEM observation (Peel & Duckett 1975) that the spermatial nucleus is apparently arrested at certain mitotic stages. It has also been reported that spermatial nuclear divisions are ordinarily completed after the attachment of uninucleate spermatia to trichogynes in

some red algae (see Fritsch 1945, p.597 for references).

Thus, fertilization in red algae includes many interesting processes for cell biologists and detailed ultrastructural studies of these events are also required (Pueschel 1990, p. 31). There are a number of reports on the ultrastructure of spermatogenesis and released spermatia as well as on the postfertilization development of the diploid carposporophyte (see Pueschel 1990, pp. 31, 32 for references). In contrast, studies on the attachment and fusion of spermatia to trichogynes are mostly limited to light microscopic observations.

Scanning electron microscopy (SEM) in Aglaothamnion (Magruder 1984) and Bangia (Cole et al. 1985) shows that spermatial appendages are specifically bound to the receptive surface of female gametes. There are a few ultrastructural studies on these events using transmission electron microscope (TEM), e.g., TEM observations on field-collected Porphyra (Hawkes 1978) and TEM figures of trichogynes before and after fertilization in Polysiphonia (Broadwater & Scott 1982). There have been no TEM studies on time-course changes in attachment and fusion of red algal gametes.

The lack of such information may be due to the difficulties in obtaining sufficient numbers of mature carpogonia in the red algae except for the bangiacean and the palmariacean algae. In the female gametophytes of the bangiacean algae, e.g., species of Bangia and Porphyra, almost all cells of the fertile portion on the thalli develop into carpogonia as judged by the formation of zygotosporangia (e.g., Hawkes 1978, Cole et al. 1985). This advantageous feature is one of the reasons that Porphyra gardneri

is the only species in which the ultrastructure of the fertilization process has been investigated (Hawkes 1978). There remain, however, certain problems concerning synchrony in carpogonial maturation. It seems difficult to distinguish mature unfertilized carpogonia from immature or vegetative cells before spermatium inoculation. Therefore, experimental studies using a sufficient number of simultaneously-matured carpogonia may be difficult in these bangiacean algae.

On the other hand, the palmariacean algae exhibit a unique life history in which haploid tetraspores develop into either macroscopic male gametophytes or microscopic female gametophytes (van der Meer & Todd 1980, van der Meer 1981). Fertilization in these algae has been observed between spermatia liberated from the male macrothallus, and a sessile carpogonia formed on the microscopic female germlings. Using these algae, it is possible to obtain a number of simultaneously-matured carpogonia on dwarf female germlings and, consequently, the palmariacean algae provide a good experimental system for studying fertilization processes in red algae.

Along the Japanese coast, the palmariacean life history has been demonstrated in Palmaria palmata O. Kuntze (Deshmukhe and Tatewaki 1990) and Halosaccion yendoi I.K. Lee (Mine and Tatewaki 1993). For the reasons mentioned above, I have chosen these palmariacean species for studies on fertilization processes in red algae. In this thesis, I present the results of recent morphological and cytochemical studies of fertilization in Palmaria palmata that will provide fundamental information for further investigation on mechanisms of fertilization processes. I de-

scribe detailed observations on spermatogenesis, liberated spermatia, trichogynes, and the attachment and fusion of these gametes of Palmaria palmata using light and epifluorescence microscopes and TEM. Several cytochemical properties that concern cellular events of fertilization are also investigated. In addition, intergeneric fertilization with Halosaccion yendoi has been attempted in order to examine taxon-specificity in the attachment and fusion of gametes.

MATERIALS AND METHODS

Preparation of male and female gametes, and spermatium inoculation

Mature sporophytes and male gametophytes of Palmaria palmata were collected from January to June of 1991, 1992 and 1993 at Charatsunai, Muroran, Hokkaido, Japan. The species of Palmaria used in the present study has been identified as Palmaria palmata O. Kuntze (Lee 1978, Sakai 1986), although the former author later decided that the northwestern Pacific Palmaria species previously known as Palmaria palmata is distinct from the Atlantic Palmaria palmata (see Hawkes & Scagel 1986). It was suspected that the northwestern Pacific 'Palmaria palmata' is conspecific with Palmaria mollis van der Meer et Bird (Hawkes & Scagel 1986) and this was supported by a recent life history study on Japanese 'Palmaria palmata' (Deshmukhe and Tatewaki 1990).

In spite of these arguments, however, the identification of the Japanese 'Palmaria palmata' requires further taxonomic investigation including cross hybridization with northeastern Pacific and Atlantic Palmaria species. Therefore I adopted Palmaria palmata as the taxonomic name of the present experimental material.

The field-collected materials were immediately transferred to the laboratory and kept at 7-10°C. The culture medium used was $ASP_{12}NTA$ (Provasoli 1963). Artificial seawater (ASW) was 450 mM NaCl, 30 mM $MgCl_2$, 16 mM $MgSO_4$, 10 mM KCl, 10 mM $CaCl_2$, and 8.25 mM Tris-HCl (pH 7.8).

A small piece (ca. 10 cm^2) of fertile sporophytic thallus

was excised, incubated in 5 mL filtered seawater on a rotary shaker for up to 1 h, and removed. Released tetraspores were pelleted by hand centrifuge and suspended in 5 mL medium. These spores were diluted to give a suspension of 4000-12000 spores per mL medium. This suspension was dispensed in 25 µL aliquots, each containing 100-300 spores, on individual coverslips and incubated in a humid atmosphere under a 45±5 $\mu mole \cdot m^{-2} \cdot s^{-1}$, continuous light provided with cool white fluorescent lamps. After 24 h, 25 µL medium was added to each coverslip.

Under these conditions, attached spores divided twice in two days and nearly half of them became fertile female gametophytes bearing a sessile carpogonium with a trichogyne. Fertilization experiments were conducted using coverslips with 3-5 day-old germlings on which more than 80% germination was confirmed.

To obtain spermatial suspension, a small piece of fertile male gametophytic thallus was excised, wiped with tissues in filtered seawater, incubated in 5 mL medium or ASW on a rotary shaker for up to 2 h, and removed. The remaining suspension of spermatia was immediately used for following experiments.

A spermatium inoculation was carried out by agitating a coverslip with tetraspore germlings in 500 µL of spermatial suspension for 15 min. Coverslips were then washed by pipetting 10 times with ca. 3 mL of medium or calcium-depleting ASW (ASW without $CaCl_2$ added with 1 mM ethylene glycol-bis(beta-aminoethyl ether) N,N,N'N'-tetraacetic acid (EGTA)) to remove indirectly entangled spermatia, and incubated in medium. Samples were fixed for DNA fluorescence microscopy or TEM observation immediately after and 5, 15, 30, 45, 60, 120 and 180 min after the onset of

spermatium inoculation.

Fluorescence microscopy

For DNA fluorescence microscopy, samples were fixed in 1% glutaraldehyde in ASW for more than 1 h, at 4°C. After rinsing with ASW, the samples were stained with 0.5 $\mu g \cdot mL^{-1}$ 4',6-diamidino-2-phenylindole (DAPI) in ASW for 1 h, rinsed with ASW, and mounted in 1:1 mixture of ASW and glycerol. Observations were carried out on Olympus BH2-RFK epifluorescence microscope using "U-excitation".

For cell wall staining, 1% (w/v) calcofluor white M2R (Fluorescent Brightener 28; Sigma, St. Louis) in ethanol was added to the medium to give a final concentration of 1-10 $\mu g \cdot mL^{-1}$, applied to specimens without fixation and examined immediately with the same epifluorescence microscope as above. Photographs were made with Neopan F (Fuji Photo Film, Tokyo) for non-fixed and DAPI-stained samples and Kodak Tri-X for calcofluor staining.

Preparation for TEM observation

Fixation for TEM was conducted at room temperature unless otherwise indicated. Method A. Samples were fixed in 3% glutaraldehyde, 2% NaCl in 0.1 M cacodylate buffer (pH 7.2) for 60 min. After rinsing with buffer containing NaCl, the samples were then postfixed in 2% osmium tetroxide in buffer containing NaCl for 30 or 60 min. The postfixed samples were washed in the buffer containing NaCl, rinsed with distilled water, and soaked in 2% aqueous uranyl acetate overnight. The samples were then dehydrat-

ed in acetone, and embedded in Spurr's resin (Spurr 1969).

Method B. Samples were fixed in 3% glutaraldehyde, 0.3 M sucrose in cacodylate buffer for 60 min. After rinsing with buffer containing 0.3 M sucrose and buffer solutions with diminishing sucrose concentration, the samples were washed in buffer and postfixed in 2% osmium tetroxide in buffer for 30 min. Postfixed samples were directly transferred to 50% acetone and soaked for 5-10 min. The samples were then incubated in 2% uranyl acetate in 70% acetone for 90 min, dehydrated in acetone, and embedded in Spurr's resin.

Method C. For preservation and enhancement of the spermatial covering and trichogyne coat, a modified method of Luft (1971) was used. Samples were fixed in 2:1 mixture of 0.1 M cacodylate buffer containing 3% glutaraldehyde, 2% NaCl and ruthenium red stock solution (1.5% in water) for 60 min. After rinsing with buffer containing NaCl, the samples were then postfixed in 2:1 mixture of buffer containing 2% osmium tetroxide, 2% NaCl and the ruthenium red stock solution for 120 min. The postfixed samples were washed in buffer containing NaCl, rinsed with water, and soaked in 2% aqueous uranyl acetate overnight. The samples were then dehydrated in ethanol, and embedded in LR white resin (London resin, Hampshire).

Method D. To observe the spermatial covering during spermatogenesis and further enhance the trichogyne coat, the following method was used. Samples were fixed in 0.1 M cacodylate buffer containing 3% glutaraldehyde and 2% NaCl for 2 h at 4°C. The samples were then washed in buffer containing NaCl, rinsed with water, and dehydrated in ethanol, and embedded in LR white resin.

Method E. Observations of membranous structures in the trichogyne cytoplasm were made on specimens postfixed with osmium tetroxide along with potassium ferricyanide. Briefly, specimens were initially fixed as by method A and then postfixed in osmium tetroxide plus 0.8% potassium ferricyanide in buffer. The en bloc staining with uranyl acetate was omitted.

Resins were polymerized at 70°C overnight. Thin sections (90-100 nm thick) were cut using a diamond knife on a Porter-Blum MT-1 ultramicrotome, stained with lead citrate (Reynolds 1963), and observed with a Hitachi H-300 transmission electron microscope. The sections of the samples prepared by method D and E were stained by both uranyl acetate (4% in water) and lead citrate.

Cytochemistry

Compounds containing vicinal glycol residues were cytochemically localized by the periodic acid-thiocarbohydrazide-silver proteinate (PATAg) test according to Roland and Vian (1991). Specimens for cytochemistry were prepared by method A for electron microscopy as above without en bloc staining with uranyl acetate.

Comparative spermatium inoculation and estimation of gamete attachment

To estimate the effect of pretreatment of gamete surfaces on gamete attachment, comparative spermatium inoculation experiments were conducted. Pretreatment procedures were described below and spermatium inoculation (5 min) was carried out as described above

using pretreated and control gametes. After washes with calcium-depleting ASW, samples were then fixed in 1% glutaraldehyde in ASW for more than 1 h at 4°C. After rinsing with ASW, the samples were mounted in a 1:1 mixture of ASW and glycerol, and the numbers of trichogynes and attached spermatia were determined under a light microscope.

Gamete attachment was estimated by counting the number of attached spermatia divided by the number of trichogynes grown on the coverslip inoculated with spermatium (designated 'spermatia/trichogynes'). In an experiment, tetraspore germlings derived from the same tetraspore suspension were used in both control and experimental duplicate coverslips and they were inoculated simultaneously with spermatia from the same spermatial suspension.

Enzymatic treatment of spermatial covering

The spermatial suspension harvested as above was diluted with ASW into 200 spermatia per µL suspension, mixed rapidly with an equal volume of ASW containing a proteolytic enzyme and kept at room temperature. Proteolytic enzymes used were Pronase E (Protease Type XIV; Sigma Chemical Co., St. Louis), trypsin (Type IX; Sigma), and papain (Wako Pure Chemicals, Tokyo). At the time of measurement, a small part of the mixture was mixed with 1/5-1/20 volume of India ink (Pellikan AG, Hanover) and the outer diameter of the transparent covering which excluded India ink was measured on 10 cells under a light microscope within 5 min. The thickness of the covering was calculated by subtracting the average cell diameter (5 µm) from the measured outer diameter and dividing by two. A stock solution of phenylmethylsulphonylfluo-

ride (PMSF; Wako; 0.2 M in ethanol) was added along with trypsin in some experiments.

When enzyme-pretreated spermatia were used for spermatium inoculation, the pretreated spermatia were washed 3 times by centrifugation (1,500 X g, 5 min) followed by resuspension in ASW before inoculation onto non-fixed trichogynes. An approximately 3 X 10^5-fold dilution of the enzyme was made after these washes and an equal amount of enzyme remaining in the pretreated inoculum was added to the control immediately before spermatium inoculation.

If fixed spermatia were subject to enzymatic treatment, the harvested spermatial suspension was mixed with an equal volume of 2% glutaraldehyde in ASW, incubated for 30 min at 4°C, and washed 3 times by centrifugation followed by resuspension in ASW. Washed samples were diluted and treated with an enzyme as above.

Periodic acid oxidation and reduction

Tetraspore germlings prepared as above were fixed in 1% paraformaldehyde in ASW for 30 min at 4°C, and washed in ASW 3 times. Samples were oxidized in 10 mM periodic acid in ASW containing 8.25 mM maleic acid (pH 4.0) for 5 min in the dark at room temperature, washed in ASW 3 times, and reduced in 0.1% sodium borohydride in ASW (pH 9.4) for 10 min in the dark. Two different controls were employed. One percent hydrogen peroxide was used in place of periodic acid for non-specific oxidation, and in the second control, reduction alone was used.

Viability test

The viability of spermatial cells was examined by both exclusion of Evan's blue (Taylor and West 1980) and fluorescence generated by hydrolysis of fluorescein diacetate (FDA; Sigma; Heslop-Harrison and Heslop-Harrison 1970). Stock solutions of Evan's blue (ca. 5% in medium) and FDA (2 $mg \cdot mL^{-1}$ in acetone) were added to cell suspensions to make final concentrations of ca. 0.5% and 4 $\mu g \cdot mL^{-1}$, respectively. Observations of FDA-stained samples were carried out on Olympus BH2-RFK epifluorescence microscope using "B-excitation". To kill the cells for negative controls of the viability test, three methods were employed; 1) spermatia were fixed in 1% glutaraldehyde in seawater for 30 min, at 4°C, 2) spermatia were treated with 0.05% saponin for 30 min, at 4°C, 3) the spermatial suspension was placed at 70°C for 10 min.

Interspecific spermatium inoculation with Halosaccion yendoi

Mature plants of Halosaccion yendoi were collected from the intertidal zone at Aikappu, Akkeshi, Hokkaido on March 23-25 of 1991. Female and male gametes were prepared as described above. Intra- and interspecific spermatium inoculation between Palmaria palmata and Halosaccion yendoi were carried out by agitating a coverslip with 5-day-old tetraspore germlings in the spermatial suspension for 15 min. Coverslips were then washed by pipetting 10 times with ca. 3 mL medium. At 180 min from spermatium inoculation, inoculated coverslips were fixed for fluorescence microscopy as above for observation of the spermatial nuclear state. Subsequent cultivation of tetraspore germlings inoculated with spermatia was carried out in PES medium (Provasoli 1966).

RESULTS

Spermatia

General morphology. Under light microscopic observations, liberated spermatia were spherical, measured ca. 5 µm in diameter, and were composed of the nuclear region and a relatively larger, colorless vacuolar region (Figs. 1, 3a). When stained with DAPI, the nucleus was observed to be highly condensed (Fig. 3b). Plastids were not detected.

TEM observations also revealed that the greater part of the cell was occupied by a condensed nucleus and large, electron-transparent vesicles that constitute the vacuolar region (Fig. 4). Small, dark-cored vesicles, endoplasmic reticulum (ER), and tubular structures were seen near the cell periphery (Figs. 4-6). The peripheral tubules were apparently continuous with the plasma membrane, and they were closely associated with peripheral ERs (Fig. 5) or with dark-cored vesicles (Fig. 6). Dictyosome-like, layered membranes were observed in the cytoplasm (Fig. 9). Dark-cored vesicles contained PATAg-positive materials (Figs. 7, 8).

The nucleus of the liberated spermatia was in prophase condition. Chromatin in the nucleus was condensed and a polar ring (PR), which is a common nucleus-associated organelle (NAO) at a division pole in red algae (Scott and Broadwater 1990), existed at both poles of the nucleus (Figs. 10, 11). An electron-dense material was detected around PRs (Fig. 11). The PRs were located above a nuclear envelope depression. Nuclear pores were seen along the depressed nuclear envelope around the PR (Fig. 12). Microtubules (MTs) were also observed around PRs in

both extranuclear and intranuclear region (Figs. 11, 12) and most of these MTs were laid toward PRs (Fig. 12). Because no cross section of MTs was observed within the nuclear pores in the tangential section of the nuclear envelopes, extracellular MTs were not continuous with intracellular MTs.

Spermatial covering. All liberated spermatia had a colorless covering which excludes carbon particles of India ink (Figs. 2, 13). Spermatial coverings were about 3 µm thick and the thickness appeared to be unchanged for at least several days after liberation. In the TEM specimen fixed by method C, a fibrous, reticulated structure was observed on the plasma membrane of spermatia (Fig. 18). In living material, cell surfaces of co-aggregated spermatia were not in direct contact with each other (Fig. 2), nor with any other objects present in the suspension, e.g., hyaline hairs shed from male macrothalli. The spermatial covering maintained its thickness when they were attached to anything other than the trichogyne.

The spermatial covering seemed to have a semi-solid, or gel-like structure. The appearance of the covering was not changed even after fixation by glutaraldehyde in seawater. Upon gradual dehydration after glutaraldehyde fixation, the covering gradually became thinner (Fig. 16). After a gradual 're-hydration' in water, the thickness was recovered and became greater than that before dehydration (Fig. 17).

The spermatial covering was degraded by proteolytic enzymes. As observed under the light microscope, the thickness of the colorless covering of non-fixed spermatia decreased in both

concentration- and time-dependent manner (Figs. 14, 15, 21, 22). In the presence of 1 mM PMSF, degradation of the covering by trypsin was partially repressed (Fig. 23). After prolonged treatment, e.g., 3 hr in 1% Pronase E, the coverings were no longer detected around spermatial cell surfaces (Fig. 15). The viability of these spermatia without coverings was confirmed (Table 1). In TEM specimens, a decrease in the covering thickness (Fig. 19) or disappearance of the covering (Fig. 20) was observed. A decrease in the covering thickness by proteolytic enzymes also occurred in glutaraldehyde-fixed spermatia (Figs. 24, 25).

The spermatial coverings were uniformly observed on all liberated spermatia and the thickness appeared to be stable. Therefore, the covering was probably produced during spermatial development before spermatium liberation. In the TEM specimens prepared by method A, electron-transparent vesicles of various sizes were observed during spermatogenesis of Palmaria palmata. Some of these vesicles were secreted from the whole surface of the plasma membrane of the spermatial cell inside the spermatangial wall (Fig. 26). The others remained within the cell to form the larger, electron-transparent vesicles in the vacuolar region of the liberated spermatium.

This secretion was observed at an early stage of spermatangial development while the spermatangium was still connected with its parent cell by a pit connection (Fig. 26). In the specimens prepared by method D, fibrous, reticulate structures apparently identical to the spermatial covering were observed both in the vesicles (Fig. 27) and in a gap formed between the spermatial plasma membrane and the spermatangial wall at a more advanced

stage (Fig. 28).

Trichogyne

Ultrastructure. Trichogynes, in contrast to spermatia, appeared to have no covering on their cell walls when observed under a light microscope (Fig. 38). But a cross section of TEM specimen fixed by method C or D showed that the cell wall surface of the trichogyne was uniformly coated with fibrous structures (Figs. 29, 30). The thickness of the trichogyne coat was about 20-30 nm or 80-100 nm in the specimens prepared by method C or D, respectively. In transverse section, the trichogyne coat appeared uniform even on the cell wall at the trichogyne apex (Fig. 32). This trichogyne coat was observed as an amorphous substance in the specimen fixed by method A or B (Fig. 51). In addition, the cell wall thickness was almost even in the method C specimens (Fig. 29) whereas it was uneven in the specimens fixed by method D or E (Figs. 30, 31).

The membranous structures of the trichogyne cytoplasm could be preserved by method E (Figs. 31, 33, 34). In a transverse section of method E specimens, the thickness of trichogyne cell wall decreased gradually toward the apex (Figs. 32, 33). Small vesicles appeared to be secreted toward the apical thin cell wall (Fig. 33). These vesicles were also observed just behind the apex, and these were associated with densely arranged ERs (Fig. 33). These ERs appeared continuous with the longitudinally arranged ERs that were usually observed in the median, not apical, portion of the trichogyne (Figs. 33, 34). In a cross section, these longitudinal ERs appeared to be arranged in a concentric

manner (Fig. 31). Dictyosomes and mitochondria were frequently observed behind the apex and the median portion (Fig. 34). Vacuoles were also observed in the median portion of the trichogyne (Fig. 31). No plastids and proplastids were observed in the trichogyne cytoplasm (Figs. 31, 33, 34).

Cytochemistry. The trichogyne coat was composed of a PATAg-positive material (Figs. 35, 36). The positive reaction of the PATAg test mostly disappeared after periodic acid oxidation followed by sodium borohydride reduction (Fig. 37). The periodic acid-sodium borohydride treatment thus appeared to destroy the PATAg-positive structure, i.e., vicinal glycol residues, of the trichogyne coat.

Gamete attachment

Morphology. Direct contact of the spermatial covering with the trichogyne coat was observed in the TEM specimens fixed immediately after spermatium inoculation (Fig. 39). In light microscopy, the cell surface of some spermatia was already attached directly to the cell wall of the trichogyne 5 minutes after spermatium inoculation (Fig. 38). The hyaline covering of these spermatia appeared to have a uniform thickness, as observed in the liberated spermatia, except for the portion where the spermatium was attached to the trichogyne. Thus, the direct attachment of spermatia to the trichogynes could occur within 5 min and the spermatial coverings were eliminated only at the site of attachment. Furthermore, the elimination of the spermatial covering and tight attachment of spermatial plasma membrane to the trichogyne

cell wall surface were observed in the TEM specimens (Fig. 39).

Inhibition of gamete attachment by degradation of gamete surfaces. The effects of pretreatment, which was expected to destroy the gamete surfaces, on the attachment of spermatia to the trichogynes were examined. A brief enzymatic pretreatment (5 min) of spermatia disrupted the ability of the spermatium to attach to the trichogyne (Tables 2, 3). The number of attached spermatia per trichogyne decreased remarkably according to the concentrations of both Pronase E and trypsin added to the pretreatment mixture. On the other hand, periodic acid oxidation followed by sodium borohydride reduction of trichogynes also inhibited gamete attachment significantly (Table 4). In contrast to an unclear difference between the controls without oxidation and those with hydrogen peroxide oxidation, a significantly smaller number of spermatia attached to the periodic acid-oxidized trichogynes.

Spermatium nuclear division

Epifluorescence microscopy. After the attachment of spermatia to trichogynes, nuclear division of the spermatium proceeded (Figs. 41-44). By epifluorescence microscopy of DAPI-stained specimens, further condensation of chromosomes (Fig. 41b), their alignment along an equatorial plate (Fig. 42b), and segregation of the chromosomes (Fig. 43b) and binucleate spermatia (Fig. 44b) were observed. All of the cell surfaces of these post-prophase spermatia were attached directly to the trichogyne cell wall.

TEM observations. Ultrastructure of the nuclear division of spermatia was examined in the specimens fixed by method B. In specimens fixed 15 min after spermatium inoculation, nuclei containing further condensed chromatin or chromosomes in disordered arrangement were observed (Fig. 45). Because no metaphase nucleus was observed in DAPI-stained specimen fixed simultaneously with those examined by TEM, it was considered that these nuclei were in prometaphase condition rather than anaphase.

In these prometaphase nuclei (Fig. 45), the nuclear envelope depression at poles was not remarkable and PRs could no longer be detected in anywhere in the serial sections throughout the cell. A part of the nuclear envelope disappeared forming a single nuclear envelope gap. Though no electron-dense materials were not seen around the gap, MTs were observed to be assembled toward the nuclear envelope region around the gap (Fig. 45).

In specimens fixed 30 min after spermatium inoculation, many metaphase or early anaphase nuclei were observed. In these nuclei, because no specialized polar structures were detectable, only a 'spindle polar region' could be determined judging from chromosome arrangement and assemblage of MTs. Figure 46 shows an early anaphase nucleus at 30 min in which beginning of chromosomes segregation can be seen. Microtubules were laid toward a somewhat prominent polar region along the inside of the nucleus and intensely condensed chromosomes, which was aligned in the equatorial plate between two poles, had begun moving toward the poles (Figs. 46, 47). Although no discrete gaps were detected, continuity of nuclear envelopes could not be demonstrated well in the polar regions, because the nuclear envelopes of these promi-

nent portions were pressed against other membranous structures (Fig. 47). Chromosomes appeared to bear kinetochores that displayed a three-layered morphology (Figs. 46-48) and several MTs were associated with a single kinetochore (Fig. 48a).

Following chromosome segregation, polar regions had become more evident than in the previous mitotic stages because the chromosomes are at opposite ends of the nucleus and their kinetochores were facing to the poles (Figs. 49, 50). The polar region of these early telophase nuclei was characterized by a large nuclear envelope gap (Fig. 49). Regeneration of nuclear envelopes within the polar gap was also found in other cells (Fig. 50). Polar rings were not detected around the early telophase nuclei.

There were two different ways of separating two derivative nuclei during early telophase. In one case, as shown in Fig. 49, the reformation of nascent nuclei was brought about by the detachment from interzonal midpiece. In this case, regeneration of nuclear envelopes along the segregated chromosomes was observed while the nuclear envelope around the interzonal midpiece remained (Fig. 49). In another case, constriction occurred in the median interzonal midpiece. Figure 50 shows an early telophase nucleus of this case. The two derivative nuclei were separated by constriction in the midpiece, around which cytoplasmic components, such as large vesicles and mitochondria, appeared between the nuclei (Fig. 50).

Observation on TEM specimens indicated that all the plasma membranes of the post-prophase spermatia were attached directly to the cell wall surface of the trichogyne. Furthermore, all of more than thirty spermatia, which remained uninucleate 180 min

after spermatium inoculation, had not attached their plasma membrane directly to the trichogynes and were morphologically similar to liberated spermatia (Fig. 51).

Spermatium cell wall formation

When stained with calcofluor, cell wall materials were not seen around liberated spermatia, but were detectable on some attached spermatia 60 min after spermatium inoculation. At this time, calcofluor fluorescence was observed around the binucleate spermatia (Fig. 52) but not around the uninucleate spermatia (Fig. 53).

As nuclear division proceeded from metaphase to telophase, the spermatial cells appeared to be rigid enough to retain the entire outline after the preparation of TEM specimens (Figs. 49, 50). A thin layer of PATAg-positive material was detected around anaphase or binucleate spermatia (Figs. 54, 55). Concomitantly, the number of the dark-cored, small vesicles seen in liberated spermatium decreased and only a few of these vesicles could be detected in the anaphase spermatium.

Gamete fusion

Epifluorescence microscopy. After cytoplasmic fusion of the binucleate spermatium with the trichogyne, the derivative nuclei (male nuclei) entered the trichogyne (Fig. 60). Male nuclei then migrated toward either the apex or the base of the trichogyne. The direction of the migration seemed to be at random.

Trichogynes could be clearly distinguished from the carpogonial base because the base was distinctly pigmented and swollen

in contrast to the uniformly limited diameter of the colorless trichogyne. I observed that three male nuclei could enter a single carpogonial base from the trichogyne. Nuclear fusion occurred between a condensed male nucleus and a large carpogonial nucleus with dispersed chromatin and a nucleolus (Fig. 61). In five replicates of the spermatium inoculation experiments, I observed that 652 spermatia had introduced their nucleus to 184 trichogynes at 180 min, and nuclear fusion was observed in 40 carpogonia at the same period. Though two of these carpogonia were invaded by two male nuclei, nuclear fusion occurred between a single male nucleus and a carpogonial nucleus (Fig. 62).

The time course of changes in nuclear behavior of the attached spermatia was examined in fertilization experiments conducted five times. The spermatial nuclear events were divided into four states that can be distinguished under a fluorescence microscope: state 1) undivided spermatial nucleus; state 2) spermatial nucleus divided into two male nuclei; state 3) one of the two male nuclei has entered into the trichogyne cytoplasm; and state 4) both male nuclei have entered into the trichogyne. Occurrence of these four states 30, 60, 120 and 180 min after spermatium inoculation are summarized in Table 5.

As a result, more than half of the attached spermatia became binucleate by 60 min though most of them were not divided at 30 min. At 180 min, about 30% of them had inserted both of the derivative nuclei inserted into the trichogyne whereas more than a third of the total spermatia remained uninucleate.

TEM observations. In the TEM specimens, the cell wall of the

trichogyne was invaded by the cytoplasm of binucleate spermatia and the invading cytoplasm expanded within the cell wall before cytoplasmic fusion (Fig. 64). Plasmogamy occurred between the expanded spermatial cytoplasm and swelling cytoplasm of the trichogyne (Fig. 65). Specialized structures for trichogyne cell wall digestion, e.g., secretion of digestive vesicles, were not detected (Fig. 63).

Passage of the male nucleus through an opening between the trichogyne and fused spermatium was not observed in TEM specimens. Several cytoplasmic components, such as large vesicles and mitochondria were left in the spermatium after the invasion of male nuclei (Fig. 66). Mitochondria and other membraneous structures were observed also at the opening between the spermatium and trichogyne cytoplasm (Fig. 66). However, because these structures were present in both trichogyne and spermatium before fertilization, their origin remained unknown.

Migrating male nuclei in a trichogyne were also observed by TEM (Figs. 67, 68), but the condensed state of chromatin, as observed in DAPI-stained migrating male nuclei, was not preserved by all the TEM preparation methods of the present study. As observed by epifluorescence, migrating male nuclei in the TEM specimens were longitudinally elongated, in an irregular or elliptical form and the width of the nucleus was about 2 µm. I did not observe two male nuclei passing each other within the limited trichogyne cytoplasm (2.5-3 µm in diameter) under an epifluorescence microscope or in TEM.

The carpogonial base of Palmaria palmata has similar cytoplasmic components to the other vegetative cells of female game-

tophyte, such as numerous plastids and starch grains, except for the carpogonial nucleus, which has dispersed chromatin and a distinct nucleolus (Fig. 71). Cell walls of female germlings did not have an obvious fibrous appearance and the wall of the female gametophyte was distinguished into two layers: inner (primary) cell wall and outer (secondary) cell wall (Fig. 70). In TEM specimens prepared by method A or B, both types of wall appeared to contain similar amorphous structures. Stainability was slightly stronger in the primary wall than in the secondary wall. The primary wall appeared outlined by electron-transparent layer (Fig. 70). The secondary wall was well-developed along the surface of the germlings but only a thin layer was detected between the cells. The trichogyne cell wall was continuous to the inner primary cell wall (Fig. 70); that is, although it was coated with the trichogyne coat, the trichogyne is the only site where the primary wall was exerted and exposed to the external environment.

Though, unfortunately, a nuclear fusion was not found, the male nucleus in a carpogonial base (Fig. 69) and the carpogonial nucleus of the same carpogonial base (Fig. 71) were observed by TEM in several carpogonia. The invading male nucleus in the carpogonial base maintained a condensed appearance and was associated with a bundle of MTs. The male nucleus had a depression or groove that was filled with MTs and some membraneous structures. The carpogonial nucleus had dispersed chromatin and a prominent nucleolus. Nuclear pores were observed in the carpogonial nucleus (Fig. 72). Polar rings were not found around the carpogonial and male nucleus in serial sectioning throughout and around the nuclei.

Intergeneric spermatium inoculation with Halosaccion yendoi

Experiments on intra- and interspecific fertilization were conducted several times and the results of a representative experiment are shown in Table 6. Data are presented as the number of trichogynes categorized into any one of the following three states: State 1) trichogynes to which no spermatium was attached; State 2) trichogynes to which at least one spermatium was attached but no cytoplasmic fusion occurred; and State 3) trichogynes fused with at least one spermatium. The occurrence of cytoplasmic fusion was judged by the invasion of a male nucleus from fused spermatium into trichogyne cytoplasm.

As shown in the table, although the ratios were invariably lower than those of intraspecific fertilization, up to 27% of trichogynes fused with the spermatia of the species of the other genus. Fusions between carpogonial and male nuclei were observed, but only a few carpogonia fused with spermatia even in intraspecific fertilization in Halosaccion yendoi. In the experiment shown in the table, the nuclei in two carpogonia of Palmaria palmata were observed to fuse with the male nucleus of Halosaccion yendoi. On the other hand, despite the numerous male nuclei invading into the trichogyne cytoplasm, no fusion was observed between Palmaria male and Halosaccion carpogonial nucleus.

Some coverslips inoculated with spermatia of the other species were subsequently incubated under the same conditions used in the life history studies of Palmaria palmata (Deshmukhe & Tatewaki 1990) and Halosaccion yendoi (Mine & Tatewaki 1993). However, further division of the carpogonium and formation of the

cell mass from carpogonia fused with spermatia was not observed after incubating for more than 2 weeks after spermatium inoculation.

DISCUSSION

Spermatium morphology

The presence of large, mucilage-containing vesicles, or vacuoles, had been reported in the spermatogenesis of many species of red algae. The appearance of the contents, modes of formation and secretion of the vesicles vary according to species (Pueschel 1990 for references, and, e.g., Scott & Dixon 1973, Kugrens 1980, Fetter & Neushul 1981). The function of these vesicles was speculated to involve the supply of a discharge force from a spermatangium and a secretion of mucilage strands, wall materials or sticky covering of liberated spermatium.

In Palmaria palmata, vesicles appeared to function in at least two ways in spermatogenesis. Firstly, the contents of vesicles secreted before spermatium liberation, judging from the present observations, may form the spermatial covering. Secretion of small vesicles within the spermatangium contributing to the spermatial wall formation had already been reported in several red algae (Scott & Dixon 1973, Peel & Duckett 1975, Kugrens 1980). The other vesicles of Palmaria palmata are never secreted out of the spermatium throughout fertilization, and serve as a wedge between the derivative nuclei of spermatial nuclear division.

Plasmalemmal tubular structures were reported on spores and spermatia in several red algae (see Pueschel 1990, p. 10 for references, Mandura et al. 1986, Scott et al. 1992). Like in Palmaria palmata spermatia, they are associated or continuous with peripheral ERs in some instances. However, close association

or continuity of the tubules with vesicles as in Palmaria palmata spermatia has not been reported. Some speculation concerning the function of vesicle-associated tubules will be presented below.

Spermatium nucleus

Both uni- and binucleate spermatia have been reported in red algae (see Goff & Coleman 1984 for references). As observed in the present study of Palmaria palmata, previous light microscopic studies indicated that the mature spermatial nucleus is in a prophase state (Grubb 1925, Fritsch 1945, p.596, Drew 1951, Magne 1952, Mumford & Cole 1977).

A condensed state of spermatial nuclei is commonly observed by TEM in red algae (Duckett & Peel 1978 for review, Kugrens 1980, Fetter & Neushul 1981). In contrast to the 'prophase-arrested' spermatial nucleus in Palmaria palmata, a TEM study of liberated spermatia in Corallina officinalis showed the spermatial nuclei arrested at metaphase or anaphase of division (Peel & Duckett 1975). The arrest of the spermatial nucleus at a later stage in Corallina suggests the possibility that spermatial nuclear division occurs, as in Choreocolax polysiphoniae and other species (Goff & Coleman 1984 for references), at an earlier stage than in Palmaria palmata. The behavior of spermatial nucleus during the fertilization of Corallina needs to be examined further.

Nuclear envelopes have been observed to be intact in most TEM studies of red algal spermatia. The present study also showed intact nuclear envelopes during spermatogenesis and in liberated spermatia. However, some earlier workers reported the absence of

a nuclear envelope in mature spermatial nuclei (Scott & Dixon 1973, Hawkes 1978). Some methods that enhance the biological membrane, e.g., method E in the present study, should be used in order to confirm the absence of the spermatial nuclear envelope in these algae.

Spermatial covering

Ultrastructural studies generally showed that liberated spermatia of red algae were covered with fibrous materials (e.g., Scott & Dixon 1973, Peel & Duckett 1975, and Broadwater et al. 1991), which were sometimes called "cell walls" (Kugrens 1974, 1980). However, because neither India ink preparation nor TEM preparation with ruthenium red and LR white was used in these study, it is impossible to compare these materials with the spermatial covering of Palmaria palmata observed in the present study.

Spermatial appendages have been reported in SEM studies of Aglaothamnion (Magruder 1984), Bangia (Cole et al. 1985) and Spyridia (Broadwater et al. 1991). The present TEM study of Palmaria palmata did not show any appendage like these species. In addition, SEM observation of Halosaccion, another genus in the Palmariaceae, also showed no projections on the smooth surface of the spermatium (Mitman & Phinney 1985).

In the present study, the cell viability and ultrastructure were not changed after an enzymatic degradation of non-fixed spermatial coverings. This degradation also occurred in fixed spermatia. Therefore, the decrease in the covering thickness observed in the presence of the enzymes does not appear to result

from damage of the covering-generating activity, if present, of the living spermatium. Furthermore, since the degradation was inhibited by a specific protease inhibitor, it was likely due to the enzymatic digestion of the protein(s) which constitutes the covering.

Though extracellular proteins have been reported (Hanic & Craigie 1969), the proteinaceous nature of spermatial coverings of red algae has not been reported. Cytochemical studies of the spermatial coverings of other red algae have shown that they consist of acidic and neutral polysaccharides (Peel and Duckett 1975, Cole et al. 1985). Using cytochemical techniques to detect proteins, Peel and Duckett (1971) reported a negative staining of the spermatial covering (as 'spermatial coat'). In Palmaria palmata, it is possible that the proteinaceous component of the spermatial covering is some kinds of glycoproteins. Further cytochemical and biochemical studies will be needed to reveal the chemical nature of the covering.

Trichogyne

In contrast to the relatively large number of studies on red algal spermatia, there are few reports on the receptive surface of female gametes of red algae. Broadwater and Scott (1982) reported that vesicles secreted in the trichogyne apex of Polysiphonia and that the trichogyne cell wall was covered by an amorphous substance which decreased in thickness from the tip to the base of trichogyne. They speculated that the substance aids in spermatial adherence. This change in trichogyne coat thickness differs from the uniform thickness of that of Palmaria palmata

observed in the present study. Cole et al. (1985) reported the relationships between histochemical nature of outer cell wall and reproductive differentiation of gametophyte in Bangia. The spermatia attached to the wall coating where sexual differentiation was morphologically initiated and the intensity of outer wall staining for sulfated polysaccharides decreased. On the trichogyne cell wall coat of Palmaria palmata, I demonstrated the PATAg-positive nature of the coat and its role in gamete attachment was discussed below in this thesis. Further studies of histochemical and biochemical nature of the coat are in progress.

Like in Polysiphonia (Broadwater & Scott 1982), the vesicle secretion at the trichogyne apex was also observed in Palmaria palmata. Because, unlike in Polysiphonia, the cell wall is very thin at the apex and its thickness gradually increases toward the median portion, it is possible that the vesicles secrete the cell wall material rather than the coating material as speculated in Polysiphonia. The ultrastructure of trichogyne cytoplasm has been studied in Polysiphonia (Broadwater & Scott 1982). The significant differences of cytoplasmic contents of Palmaria trichogynes from those of Polysiphonia are the longitudinal, concentric arrangement of ERs and the absence of plastids and proplastids.

Gamete attachment

The present study is the first detailed TEM documentation of the gamete attachment process of red algae. There have been several SEM studies on red algal gamete attachment (Magruder 1984, Cole et al. 1985, Mitman & Phinney 1985). The two examples given above, in the bangiacean and ceramiacean algae, showed spe-

cialized appendages (or 'corns') on the spermatia which were responsible for the initial binding to the receptive surface of female gamete. The Bangiaceae and the Ceramiaceae are two of the most phylogenetically remote taxa, and, therefore, it might be assumed that specialized spermatial appendages are a common attachment apparatus in red algae. However, a previous SEM study (Mitman & Phinney 1985) and the present TEM study showed that spermatia of the palmariacean algae have no appendage on the surface throughout the fertilization process. Further strict comparisons of the morphogenesis, the stability and detailed morphology of the specialized spermatial appendages of different taxa in red algae are necessary.

The spermatia of Palmaria palmata do not possess flagella, and I did not observe any amoeboid movement as reported in spores of Erythrocladia (Nichols & Lissant 1967). Furthermore, the initial processes of fertilization of Palmaria palmata (i.e., calcium depletion-insensitive, fixed attachment and localized elimination of spermatial covering) commenced immediately after spermatium inoculation to the trichogyne. It is likely that Palmaria palmata spermatia are essentially non-motile and that the recognition and attachment of passively moving spermatia to the sessile non-motile carpogonium is governed principally by adhesive surface materials of both gametes.

It is probable that the inhibition of gamete attachment by brief enzymatic pretreatment as shown in Table 2 and 3 was caused by degradation of the outermost layer of the covering. On the other hand, it is also possible that other important membrane-bound proteins were disrupted by the proteolytic enzymes and this

had a secondary effect on the spermatial attachment as argued in gamete adhesion of Chlamydomonas (Goodenough 1991).

The PATAg-positive compounds of the trichogyne coat appear to be essential for gamete attachment since attachment was markedly inhibited by specific chemical degradation of vicinal glycols of the coat. The PATAg-positive entity can be interpreted in various ways (Roland and Vian 1991), but the great majority of positive compounds are polysaccharides containing 1-4 linkages. There have been many examples that indicate lectin-polysaccharide interaction in gamete recognition in animals (Rosati 1985, O'Rand 1988 for reviews) and brown algae (Callow 1985, for review). If the trichogyne PATAg-positive compounds are polysaccharides, it is likely that the complementary proteinaceous compound of the surface of the spermatial covering is a lectin that binds to the trichogyne coat polysaccharide. As in the studies of fertilization in Fucus (Bolwell et al. 1979), an examination of the effect of lectins or specific glycosidases on gamete attachment will provide further information on the adhesive trichogyne coat containing vicinal glycols.

The spermatial covering of Palmaria palmata was attached to the trichogyne cell wall coat immediately after spermatium inoculation. The initial attachment was strong enough to be maintained even after chemical fixation, rinsing and embedding for TEM observations. This is in contrast to the non-specific binding of indirectly entangled spermatia which was easily destroyed by washes in calcium-depleting ASW. The co-aggregation or non-specific entanglement of the spermatia is probably mediated by EGTA-sensitive strands (Fetter and Neushul 1981) or sheets (Guiry

1974) of extracellular mucilage. Moreover, the specific interaction between the spermatial covering and trichogyne coat involves not only organ- and taxon-specific binding but also rapid, localized elimination of the spermatial covering leading to the direct attachment of gametes and the consequent events of fertilization.

Nuclear division

Nuclear division of uninucleate spermatia has been observed by light microscopy in several species of red algae. After liberation of spermatia, division occurs before gamete attachment in some species, e.g., Choreocolax (see Goff & Coleman 1984). However, as observed in the present study on Palmaria palmata, spermatial nuclear divisions were ordinarily found 'after' attachment of uninucleate spermatia to trichogynes in Nemalion and Batrachospermum (see Fritsch 1945, p.597 for references).

In contrast to the condensed state of the spermatial or male nucleus throughout the fertilization processes in Choreocolax (Goff & Coleman 1984) or in the present study, Hawkes (1978) observed decondensation of the spermatial nucleus after attachment to the prototrichogyne. It is possible that the decondensation of spermatial nucleus is, in part, due to the absence of nuclear envelope. Hawkes (1978) speculated that the decondensation occurs in order to 'code for an enzyme required to make the fertilization canal'. Examination whether gene expression is required for the canal formation after the gamete attachment in Porphyra is necessary.

The present study is the first TEM observation of spermatial nuclear division in red algae. TEM figures of a spermatial nucle-

us arrested at metaphase or anaphase have been shown previously (Peel & Duckett 1975). The nuclear division of spermatia of Palmaria palmata shared several ultrastructural features with somatic cell division of other red algae (reviewed by Scott and Broadwater 1990), but it was immediately followed by fusion with a trichogyne.

Perinuclear ER was not particularly observed and the continuity between the nuclear envelope and peripheral ER was not detected. Like in most red algae the nuclear envelope remained throughout the nuclear division except for a polar gap formed at prometaphase. Although not clearly demonstrated yet in the present study, the gap may be present during metaphase and anaphase since no red alga so far studied has totally enclosed pole at these stages.

It was an unexpected result that the segregated chromosomes in early anaphase can be separated by either constriction of interzonal midpiece or detachment from the midpiece. The latter is the only case hitherto reported in red algae (Scott et al. 1980, Scott and Broadwater 1990, Scott et al. 1992). McDonald (1972) showed a TEM micrograph indicating midpiece constriction separating derivative nuclei, but a negative decision on this observation was presented using intensive serial sectioning (Scott et al. 1980). On the midpiece constriction in Palmaria palmata, however, the observations were based on serial sectioning throughout the cell and the midpiece was detected only along the constriction. Therefore, it was concluded that the derivative nuclei could be separated by a midpiece constriction in the spermatium of Palmaria palmata.

Even when the present observations given above were reliable, the duality in a mitotic event may still seem unusual. The midpiece constriction is apparently caused by the intrusion of other organelles, e.g., large vesicles and mitochondria. It is possible that these organelles move passively in the limited volume of cytoplasm of the spermatium rather than under a control of a positive physiological mechanism. If so, it can be a frequent phenomenon that the midpiece constriction takes place before the detachment of the midpiece from the nascent nuclei.

Disappearance of polar ring

The polar ring observed in the present study was morphologically similar to that of prophase nucleus in Palmaria palmata (Scott & Broadwater 1990). It disappeared before late prophase of spermatial nuclear division. This is contrary to the case in some red algae, e.g., Polysiphonia, where polar rings were observed to be persistent through interphase as well as in mitotic phases, and they were introduced to derivative cells from the parent cell in a semi-conservative manner (Scott et al. 1980, Scott & Broadwater 1990). But a similar phenomenon to that in the spermatium of Palmaria palmata was reported in vegetative cells of Apoglossum, in which polar rings degenerated during metaphase (Dave & Godward 1982).

Because the nuclear division of vegetative cells of Palmaria palmata is not fully studied yet, it is possible that the disappearance of the polar ring is a specific phenomenon for gametes in this alga. Neither carpogonial nuclei nor male nuclei invading into the carpogonial base were associated with a polar ring, and

it is very likely, therefore, that they fuse without a polar ring. In the fertilization of other lower eukaryotes, centrioles or NAOs were observed to be persistent during the fertilization process (e.g., Byers & Goetsch 1975, Motomura 1989, 1992). The disappearance of the polar ring before gamete fusion provides new information on the function of the polar rings and their phylogenetic relationship with the other NAOs.

Prophase arrest

In Palmaria palmata, the strictly prophase-arrested nucleus of the liberated spermatium proceeded to post-prophase stages only after attachment of the plasma membrane to the trichogyne surface. This indicates the presence of a signal transduction mechanism that converts an extracellular stimulus (attachment of the plasma membrane to the trichogyne surface) to an intracellular event (post-prophase progression of nuclear division). Fertilization of Palmaria palmata could be a potentially useful experimental system for studying the signal transduction mechanism of red algae and control of mitotic progression in lower eukaryotes.

There is currently great interest in the mechanisms controlling cell cycle progression and a number of keys may reveal the post-prophase progression mechanism in Palmaria spermatia. For example, fully grown amphibian eggs are arrested at meiotic prophase I and the arrest is released by activation of cytoplasmic 'maturation-promoting factor' (Shibuya & Masui 1988), and adenosine 3',5'-cyclic monophosphate has an antagonistic effect on hormone-induced meiosis reinitiation (Schorderet-Slatkine & Baulieu 1982). It is generally known that the level of cytoplas-

mic free calcium ions alters during several mitotic events including post-prophase progression (Poenie et al. 1985, Steinhardt & Alderton 1988). Along these lines, further investigations are in progress to elucidate the mechanisms involved in the progression of nuclear division of Palmaria palmata spermatia after direct attachment to the trichogyne.

Spermatial cell wall formation

The completion of nuclear division is accompanied by formation of cell wall detected as calcofluor- and PATAg-positive substances. During fertilization of Porphyra, a thin layer of wall material was seen around spermatia attached to the prototrichogyne before cytoplasmic fusion (Hawkes 1978). In Palmaria palmata, judging from their concomitant decrease, and identity of the contents, the small, dark-cored vesicles may contribute the cell wall formation. Moreover, it is possible that the peripheral tubules, which are closely associated with both the plasma membrane and the small vesicles, are concerned with secretion of cell wall material secretion. As pointed out by Pueschel (1990. p.10), the continuity between the tubule and the external environment must be confirmed using heavy metal markers.

There have been few examples of actual demonstration of cell structure involved in formation of cell coverings in red algae. Ultrastructural autoradiography of a unicellular red alga has demonstrated that sulfation of extracellular mucilage was carried out in dictyosomes (Evans et al. 1974). These sulfated polysaccharides processed through dictyosomes are probably secreted via vesicle secretion. More recent ultrastructural study of Erythro-

cladia showed putative microfibril-synthesizing complexes in the plasma membrane, which are apparently similar to those of chlorophycean algae (Tsekos & Reiss 1992). The contribution of the vesicle and plasma membrane tubules to the spermatial cell wall formation in Palmaria spermatia has not been fully demonstrated in the present study. However, the wide distribution of this structure in red algae suggests that the plasma membrane tubule is one of the major structures involved in formation of cell coverings in red algae.

Short-lived, tubular plasmalemmal structures have been observed in tetraspores of Palmaria palmata (Mandura et al. 1986). After attachment to the substratum, the liberated tetraspore of Palmaria palmata develops calcofluor-positive material and commences germination, i.e., cell division (Figs. 56-59). Though presence of the PATAg-positive vesicles was not confirmed in tetraspores of Palmaria palmata, triggering of cell wall formation and nuclear division after attachment of the cell to an 'appropriate' substratum is an interesting analogy between the spermatial nuclear division and tetraspore germination.

Gamete fusion

Carpogonia have been studied previously using TEM in two species, Porphyra gardneri (Hawkes 1978) and Polysiphonia harveyi (Broadwater & Scott 1982). The most distinct differences in the cytoplasmic component of the carpogonia of these examples are the degree of plastid development and the presence (or absence) of starch grains. Fully developed plastids and numerous starch grains were observed in Porphyra, but only proplastids and no

starch grains were detected in Polysiphonia. Despite the similarity in an external appearance (i.e., distinction between trichogyne and carpogonial base), the ultrastructure of the carpogonium of Palmaria palmata observed in the present study is quite different from that of Polysiphonia.

On the other hand, prominent plastid development and numerous starch grains in the carpogonium or carpogonial base are features common to Porphyra and Palmaria. This is not surprising in consideration of recent arguments that the order Palmariales is among the most primitive groups of red algae (Pueschel & Cole 1985, Guiry 1987).

The ultrastructure of the gamete fusion process of red algae had been observed by Hawkes (1978) in field-collected Porphyra gardneri. In this instance, the 'spermatial nuclear material' was transferred to the carpogonium via a narrow, extended fertilization canal. In Porphyra, the nuclear material seemed to be the first cytoplasmic component being transferred into the fertilization canal, and other components, such as proplastids, followed the nuclear material into the canal (Hawkes 1978). In contrast, the cytoplasm of the attached spermatium of Palmaria palmata formed an expanded opening within the thin trichogyne cell wall before cytoplasmic fusion and male nucleus invasion. This expansion of the opening between spermatium and trichogyne cytoplasm may assure nuclear transfer with minimum constriction of the invading male nucleus.

The present study is the first ultrastructural report of the male (spermatial) nucleus invading the carpogonium of red algae. The most striking feature of the male nucleus invading in the

carpogonial base of Palmaria palmata is the association of MTs. During fertilization of the brown alga Fucus distichus, nuclear migration of the male pronucleus toward the co-existing egg nucleus is inhibited by MT inhibitors (Brawley 1979), implying that MTs play an indispensable role for male nuclear migration in this alga. The remarkable association of MTs with the male nucleus in the carpogonial base of Palmaria palmata is similarly suggestive of the function of MTs in the migration of male nucleus to the carpogonial nucleus.

Polyspermy block

It has previously been reported that two or more male (or spermatial) nuclei from one or more spermatia may enter into a trichogyne (e.g., Goff & Coleman 1984, O'Kelly & Baca 1984). Even when only one spermatium attached to a trichogyne in the fertilization of Palmaria palmata, the spermatial nucleus divides into two male nuclei and both of them may enter the cytoplasm of the trichogyne. Thus, there must be a mechanism that allows the fusion of only one male nucleus with a carpogonial nucleus.

Judging from the present observations, it is likely that male nuclei cannot pass each other within the limited diameter inside the trichogyne and the direction of male nucleus migration seems to be random. Therefore, even when numerous male nuclei entered the trichogyne as observed in the present experiments, only a limited number of male nuclei can enter into the carpogonial base from the trichogyne.

Deshmukhe and Tatewaki (1990) reported that the lower portion of the trichogyne of fertilized carpogonia of Palmaria

palmata became narrower, forming a septum to prevent the entrance of an additional male nucleus. As a general rule in fertilization of red algae, a septum formation should be completed before the 'walling off' of the trichogyne, which is a common phenomenon during further development of fertilized carpogonia of red algae (Pueschel 1990). The present observation of TEM specimens failed to show such a septum, and an examination of specimens incubated for a far longer period is necessary to judge the significance of septum formation in the polyspermy block.

Intergeneric cross with Halosaccion yendoi.

A qualitative estimation of gamete attachment between related species and genera of ceramiacean algae has been reported (Magruder 1984). The present study is the first comparative quantification of gamete attachment between red algae of different taxa. Gamete attachment between different taxa was invariably lower than that of the intraspecific controls. Morphological and cytochemical observations described previously in this thesis have shown that the spermatial covering and the trichogyne coat mediate the attachment of these non-flagellated gametes. The weakness of heterologous gamete attachment must be due to the divergence in the biochemical nature of these gamete surfaces between the two taxa.

Both cytoplasmic and nuclear fusion in the intergeneric fertilization were invariably less frequent than in intraspecific controls, but were readily observed in the present study. In contrast to this, no binding was observed between the gametes of Aglaothamnion neglectum (Ceramiaceae) and other species of relat-

ed genera (Magruder 1984). Thus the stages where the fertilization between different genera is blocked are different between the Palmariaceae and Ceramiaceae. This difference may be related to the absence of any specialized appendage on the spermatium in palmariacean algae (e.g., Palmaria and Halosaccion). These appendages have been reported in species of Ceramiaceae (Magruder 1984, Broadwater et al. 1991) and bind specifically to trichogynes (Magruder 1984).

Among red algae, it is generally recognized that the development of interspecific hybrids is, if it occurs at all, abnormal and often results in sterile progeny (van der Meer 1988, p. 517). There have been several studies on intra- and interspecific hybridization in Palmaria spp. (van der Meer & Bird 1985, van der Meer 1987). Experimental hybridization between northeast and northwest Atlantic Palmaria palmata yielded intraspecific hybrids with greatly reduced fertility (van der Meer 1987). The developmental deficiency of hybrid zygotes of red algae, such as the abortive intergeneric zygote in the present study, may be due to genomic incompatibility (van der Meer 1988), which assures reproductive isolation between Palmaria palmata and Halosaccion yendoi in natural populations along the Hokkaido coast.

In contrast to the frequency of gamete fusion between Palmaria palmata and Halosaccion yendoi, not a single 'fertilization' was detected even in intrageneric crosses between Atlantic Palmaria palmata and Palmaria mollis (van der Meer & Bird 1985). Though no crosses with species of different genera have been attempted in these Atlantic species, it is likely that fertilization would not occur with more remote taxa, e.g., species of the

genus Halosaccion. Further investigations of inter- and intrageneric fertilization with species of Palmaria of northeast Pacific or north Atlantic coasts will reveal whether species differentiation in Palmaria was accompanied by barriers to heterologous fertilization at the level of gamete fusion.

SUMMARY

Structures and processes (i.e., spermatogenesis, liberated spermatium, trichogyne, gamete attachment, spermatial nuclear division and cell wall formation, and gamete fusion) in fertilization of the red alga Palmaria palmata were observed using light, epifluorescence and transmission electron microscopes. Precise time-course examination was possible using this alga, because it forms rapidly-maturing microscopic female gametophytes and macroscopic male gametophyte liberating spermatia vigorously. In addition, attempts of intergeneric fertilization with Halosaccion yendoi I.K. Lee were made in order to examine the taxon-specificity of gamete attachment and fusion.

The results obtained are summarized as follows.

1. Liberated spermatium has a prophase nucleus with a division pole marked with a pair of polar rings. Dark-cored, small vesicles with PATAg-positive contents are observed in cell periphery and these vesicles are apparently connected to plasma membrane via plasma membrane tubules.

The protoplast of spermatium is covered with a hyaline, 3 µm thick covering. The spermatial covering appeared as fibrous, reticulated matrix when observed by TEM and is apparently secreted during spermatogenesis before liberation of spermatium. The spermatial covering is degraded by certain proteolytic enzymes.

2. In the cytoplasm of trichogyne, concentric, longitudinally-arranged ERs, dictyosomes and mitochondria are observed. Secretion of small vesicles apparently derived from ERs is detected in the apex of trichogyne. The cell wall of trichogyne is

covered with PATAg-positive, fibrous coat.

3. The attachment of spermatium to trichogyne can be established very rapidly after spermatium inoculation. Immediately after spermatium inoculation, the attachment of the surface of spermatial covering to the trichogyne coat become stable enough to be maintained after TEM preparation. In 5 min after inoculation, the spermatial covering is eliminated completely only at the site of attachment resulting in the direct attachment of spermatial plasma membrane to the trichogyne cell wall surface.

The gamete attachment is effectively inhibited by brief pretreatment of spermatia with proteolytic enzymes as well as by destruction of PATAg-positive compound of trichogyne coat with periodic acid oxidation followed by sodium borohydride reduction.

4. After the direct attachment of gametes, prophase-arrested spermatial nucleus proceeds the nuclear division. Nuclear envelope remained intact throughout the nuclear division and, during degeneration of interzonal midpiece at late anaphase and early telophase, both invasion of organelles (i.e., large vesicles, mitochondria) and reformation of nuclear envelopes occur between the derivative nuclei. The nuclear envelope polar gap is formed from prometaphase to telophase. Polar rings disappears before prometaphase.

The completion of spermatial nuclear division (telophase) is observed in 45 min after spermatium inoculation. In the TEM specimens at 180 min, all the spermatia with nucleus remained at early prophase have their plasma membrane not attached directly to the trichogyne wall surface. This indicates the direct attachment of gametes is necessary to the post-prophase progression of

spermatial nuclear division.

As spermatial nuclear division proceeds, cell wall material, recognized as calcofluor- and PATAg-positive material, is formed around the spermatium. Concomitantly, the small, PATAg-positive vesicles decreased in the cytoplasm, implying that the vesicle contents is the source of the cell wall material.

5. After completion of spermatial nuclear division, the cytoplasm of the binucleate spermatium invades into and expands within the trichogyne cell wall before cytoplasmic fusion of gametes. Both of the two derivative nuclei (male nuclei) of spermatial nuclear division enter the trichogyne cytoplasm and migrate toward either the apex or the base of trichogyne. The trichogyne fused with multiple spermatia and many male nuclei are observed to enter into the trichogyne cytoplasm. However, probably because the limited diameter of the trichogyne and random migration of male nuclei, the number of male nuclei that invade into a carpogonial base is no more than three as far as observed.

The male nucleus invading into the carpogonial base is associated with a number of MTs but not with a polar ring. The male nucleus maintains its condensed state until nuclear fusion with a carpogonial nucleus. The carpogonial nucleus is not associated with the polar ring.

6. Though the ratio is invariably lower than intraspecific controls, the attachment and fusion between gametes of Palmaria palmata and Halosaccion yendoi were readily observed in the intergeneric spermatium inoculation experiments. The nuclear fusion of Halosaccion male and Palmaria carpogonial nuclei was observed but no zygote development was detected.

REFERENCES

Bolwell, G. P., Callow, J. A., Callow, M. E. and Evans, L. V.
1979. Fertilization in brown algae. II. Evidence for lectin -sensitive complementary receptors involved in gamete recognition in Fucus serratus. J. Cell Sci. 36:19-30.

Brawley, S. H. and Quatrano, R. S.
1979. Effects of microtubule inhibitors on pronuclear migration and embryogenesis in Fucus distichus (Phaeophyta). J. Phycol. 15:266-272.

Broadwater, S. T. and Scott, J.
1982. Ultrastructure of early development in the female reproductive system of Polysiphonia harveyi Bailey (Ceramiales, Rhodophyta). J. Phycol. 18:427-441.

Broadwater, S. T., Scott, J. L. and West, J. A.
1991. Spermatial appendages of Spyridia filamentosa (Ceramiaceae, Rhodophyta). Phycologia 30:189-195

Byers, B. and Goetsch, L.
1975. Behavior of spindles and spindle plaques in the cell cycle and conjugation of Saccharomyces cervisiae. J. Bacteriol. 124:511-523.

Callow J. A.
1985. Sexual recognition and fertilization in brown algae. J. Cell Biol. suppl. 2: 219-232.

Cole, K. M., Park, C. M., Reid, P. E. and Sheath, R. G.
1985. Comparative studies on the cell walls of sexual and asexual Bangia atropurpurea (Rhodophyta). I. Histochemistry of polysaccharides. J. Phycol. 21:585-592.

Dave, A. J. and Godward, M. B. E.

1982. Ultrastructural studies in the Rhodophyta. I. Development of mitotic spindle poles in Apoglossum ruscifolium, Kylin. J. Cell Sci. 58:345-362.

Deshmukhe, G. V. and Tatewaki, M.

1990. The life history and evidence of the macroscopic male gametophyte in Palmaria palmata (Rhodophyta) from Muroran, Hokkaido, Japan. Jpn. J. Phycol. 38:215-222.

Dixon, P. S.

1973. Biology of the Rhodophyta. Hafner, New York.

Drew K. M.

1951. Rhodophyta. In G. M. Smith [ed.], Manual of Phycology. pp. 167-191. Chronica Botanica Co. Waltham, Mass.

Duckett, J. G. and Peel M. C.

1978. The role of transmission electron microscopy in elucidating the taxonomy and phylogeny of the Rhodophyta. In D. E. G. Irvine and J. H. Price [eds.], Modern Approaches to the Taxonomy of Red and Brown Algae. pp. 157-204. Academic Press, London.

Evans, L. V., Callow, M. E., Percival, E. and Fareed, V.

1974. Studies on the synthesis and composition of extracellular mucilage in the unicellular red alga Rhodella. J. Cell Sci. 16:1-21.

Fetter, R. and Neushul, M.

1981. Studies on developing and released spermatia in the red alga, Tiffaniella snyderae (Rhodophyta). J. Phycol. 17:141-159.

Fritsch, F. E.

1945. The structure and reproduction of algae. vol. II. 939pp.+xii. Cambridge University Press, Cambridge.

Goff, L. J. and Coleman, A. W.

1984. Elucidation of fertilization and development in a red alga by quantitative DNA microspectrofluorometry. Dev. Biol. 102:173-194.

Goodenough, U. W.

1991. Chlamydomonas mating interactions. In M. Dworkin [ed.], Microbial Cell-Cell Interactions. American Society for Microbiology, Washington.

Grubb, V. M.

1925. The male organs of the Florideae. J. Linn. Soc. (Bot.) 47:177-255.

Guiry, M. D.

1974. A preliminary consideration of the taxonomic position of Palmaria palmata (Linnaeus) Stackhaus = Rhodymenia palmata (Linnaeus) Greville. J. Mar. Biol. Assoc. U. K. 54:509-528.

Guiry, M. D.

1987. The evolution of life history types in the Rhodophyta: an appraisal. Cryptogam. Algol. 8:1-12.

Hanic, L. A. & Craigie, J. S.

1969. Studies on the algal cuticle. J. Phycol. 5:89-102

Hawkes, M. W.

1978. Sexual reproduction in Porphyra gardneri (Smith et Hollenberg) Hawkes (Bangiales, Phodophyta). Phycologia 17:329-353.

Hawkes, M. W. & Scagel R. F.

1986. The marine algae of British Columbia and northern Washington: division Rhodophyta (red algae), class Rhodophyceae, order Palmariales. Can. J. Bot. 64:1148-1173.

Heslop-Harrison, J. and Heslop-Harrison Y.

1970. Evaluation of pollen viability by enzymatically induced fluorescence; intracellular hydrolysis of fluorescein diacetate. Stain Technol. 45:115-120.

Hommersand, M. H. and Fredericq, S.

1990. Sexual reproduction and cystocarp development. p.305-345. In K. M. Cole and R. G. Sheath [eds.], Biology of red algae. Cambridge University Press, Cambridge.

Kim, G. H. and Fritz, L.

1993. Gamete recognition during fertilization in a red alga Antithamnion nipponicum. J. Phycol. 29, suppl. No. 3:19.

Kugrens, P.

1974. Light and electron microscopic studies on the development and liberation of Janczewskia gardneri Setch. spermatia (Rhodophyta). Phycologia 13:295-306.

Kugrens, P.

1980. Electron microscopic observations on the differentiation and release of spermatia in the marine red alga Polysiphonia hendryi (Ceramiales, Rhodomelaceae). Amer. J. Bot. 67:519-528.

Lee, I. K.

1978. Studies on Rhodymeniales from Hokkaido. J. Fac. Sci. Hokkaido Univ. Ser. 5. 11:1-194.

Luft, J. H.

1971. Ruthenium red and violet I. Chemistry, purification,

methods of use for electron microscopy and mechanism of action. Anat. Rec. 171:347-368.

Magne, F.

1952. La structure du noyau et le cycle nucleaire chez le Porphyra linearis Greville. C. R. Acad. Sci. Paris 234:986-988.

Magne, F.

1987. La tetrasporogenese et le cycle de developpement des Palmariales (Rhodophyta): une nouvelle interpretation. Cryptogam. Algol. 8:273-280.

Magruder, W. H.

1984. Specialized appendages on spermatia from the red alga Aglaothamnion neglectum (Ceramiales, Ceramiaceae) specifically bind with trichogynes. J. Phycol. 20:436-440.

Mandura, A., Boney, A. D. and Bowes, B. G.

1986. Tubular plasmalemmal structures in newly released spores of some red algae. Nova Hedwigia 42:277-282.

McDonald, K.

1972. The ultrastructure of mitosis in the marine alga Membranoptera platyphylla. J. Phycol. 8:156-166.

Mine, I. and Tatewaki, M.

1993. Life history of Halosaccion yendoi I.K. Lee (Palmariales, Rhodophyta) and interspecific spermatium inoculation with Palmaria sp. from Hokkaido, Japan. Jpn. J. Phycol. 41:123-130.

Mitman, G. G. and Phinney, H. K.

1985. The development and reproductive morphology of Halosaccion americanum I. K. Lee (Rhodophyta, Palmariales). J. Phycol.

21:578-584.

Motomura, T.

1990. Ultrastructure of fertilization in Laminaria angustata (Phaeophyta, Laminariales) with emphasis on the behavior of centrioles, mitochondria and chloroplasts of the sperm. J. Phycol. 26:80-89.

Motomura, T.

1992. Disappearance of centrioles derived from female gametes in zygotes of Colpomenia bullosa (Phaeophyceae). Jpn. J. Phycol. 40:207-214.

Mumford, Jr., T. F. and Cole, K.

1977. Chromosome numbers for fifteenspecies in the genus Porphyra (Bangiales, Rhodophyta) from the west coast of North America. Phycologia 16:373-377.

Nichols, H. W. and Lissant, E. K.

1967. Developmental studies of Erythrocladia Rosenvinge in culture. J. Phycol. 3:6-18.

O'Kelly, C. J. and Baca, B. T.

1984. The time course of carpogonial branch and carposporophyte development in Callithamnion cordatum (Rhodophyta, Ceramiales). Phycologia 23:407-417.

O'Rand, M. G.

1988. Sperm-egg recognition and barriers to interspecies fertilization. Gamete Res. 19:315-328.

Peel, M. C. and Duckett, J. G.

1975. Studies of spermatogenesis in the Rhodophyta. Biol. J. Linn. Soc. vol. 7, suppl. 1:1-13.

Poenie, M., Alderton, J., Tsien, R. Y. and Steinhardt, R. A.

1985. Changes of free calcium levels with stages of the cell division cycle. Nature 315:147-149.

Provasoli, L.

1963. Growing marine seaweeds. In D. DeVirville and J. Feldmann [eds.], Proc. Fourth Int. Seaweed Symp. pp.9-17. Pergamon Press.

Provasoli, L.

1966. Media and prospects for the cultivation of marine algae. In A. Watanabe and A. Hattori [eds.], Culture and Colections of Algae. pp. 63-75. Japanese Society of Plant Physiologists, Tokyo.

Pueschel, C. M.

1990. Cell structure. In K. M. Cole and R. G. Sheath [eds.], Biology of the red algae. pp. 7-41. Cambridge University Press.

Pueschel, C. M. and Cole, K. M.

1982. Rhodophycean pit plugs: an ultrastructural survey with taxonomic implications. Am. J. Bot. 69:703-720.

Reynolds, E. S.

1963. The use of lead citrate at high pH as an electron opaque stain in electron microscopy. J. Cell Biol. 17:208-212.

Roland, J. C. and Vian, B.

1991. General preparation and staining of thin sections. In J. L. Hall and C. Hawes [eds.], Electron microscopy of plant cells. pp. 1-66. Academic Press, London.

Rosati, F.

1985. Sperm-egg interaction in ascidians. In C. B. Metz & A. Montroy [eds.] Biology of fertilization. pp. 361-338.

Academic Press, New York.

Sakai, Y.

1986. A list of marine algae from the vicinity of the Institute of Algological Research of Hokkaido University, Muroran, Japan. Sci. Pap. Inst. Algol. Res., Fac. Sci., Hokkaido Univ. 8:1-30.

Schorderet-Slatkine, S. and Baulieu, E.-E.

1982. Forskolin increases cAMP and inhibits progesterone induced meiosis reinitiation in Xenopus laevis oocytes. Endocrinology 111:1385-1387.

Scott J.

1983. Mitosis in the freshwater red alga Batrachospermum ectocarpum. Protoplasma 118:56-70.

Scott, J. and Broadwater, S.

1990. Cell division. In K. M. Cole and R. G. Sheath [eds.], Biology of the red algae. pp. 123-145. Cambridge University Press, Cambridge.

Scott, J., Bosco, C., Schornstein, K. and Thomas, J.

1980. Ultrastructure of cell division and reproductive differentiation of male plants in the Florideophyceae (Rhodophyta): cell division in Polysiphonia. J. Phycol. 16:507-524.

Scott, J. L., Broadwater, S. T., Saunders, B. D., Thomas, J. P. and Gabrielson, P. W.

1992. Ultrastructure of vegetative organization and cell division in the unicellular red alga Dixoniella grisea gen. nov. (Rhodophyta) and a consideration of the genus Rhodella. J. Phycol. 28:649-660.

Scott, J. L. and Dixon, P. S.

1973. Ultrastructure of spermatium liberation in the marine red alga Ptilota densa. J. Phycol. 9:85-91.

Shibuya, E. K. and Masui, Y.

1988. Stabilization and enhancement of primary cytostatic factor (CSF) by ATP and NaF in amphibian egg cytosols. Dev. Biol. 129:253-264.

Spurr, A. R.

1969. A low viscosity epoxy resin embedding medium for electron microscopy. J. Ultrastruc. Res. 26:31-43.

Steinhardt, R. A. and Alderton, J.

1988. Intracellular free calcium rise triggers nuclear envelope breakdown in the sea urchin embryo. Nature 332:364-366.

Taylor, J. A. and West, D. W.

1980. The use of Evan's blue stain to test the survival of plant cells after exposure to high salt and high osmotic pressure. J. Exp. Bot. 31:571-576.

Tsekos, I. and Reiss, H. D.

1992. Occurence of the putative microfibril-synthesizing (linear terminal complexes) in the plasma membrane of the epiphytic marine red alga Erythrocladia subintegra Rosenv. Protoplasma 169:57-67.

van der Meer, J. P.

1981. The life history of Halosaccion ramentaceum. Can. J. Bot. 59:433-436.

van der Meer, J. P.

1987. Experimental hybridizations of Palmaria palmata (Rhodophyta) from the northeast and northwest Atlantic Ocean. Can.

J. Bot. 65:1451-1458.

van der Meer, J. P.

1988. The generic improvement of algae: progress and prospects. In C. A. Lembi and J. R. Waaland [eds.], Algae and Human Affairs. Cambridge University Press, Cambridge.

van der Meer, J. P. and Todd, E. R.

1980. The life history of Palmaria palmata in culture. A new type for the Rhodophyta. Can. J. Bot. 58:1250-1256.

van der Meer, J. P. and Bird, C. J.

1985. Palmaria mollis stat. nov.: a newly recognized species of Palmaria (Rhodophyceae) from the northeast Pacific Ocean. Can. J. Bot. 63:398-403.

Table 1. Viability test of spermatia after complete degradation of covering.

treatment	FDA	Evan's blue
none	+	–
1% pronase E, 180 min	+	–
1% trypsin, 180 min	+	–
1% glutaraldehyde, 30 min	–	+
0.05% saponin, 30 min	–	+
70°C, 10 min	–	+

Table 2. Effect of Pronase E preincubation (5 min) of spermatia on attachment to untreated trichogynes.

pretreatment	No. of trichogynes	No. of attached spermatia	spermatia /trichogynes
control	156	525	3.36
	165	660	4.00
0.01% (w/v) Pronase E	118	73	0.62
	137	41	0.29
0.1% Pronase E	168	18	0.11
	187	20	0.11

Table 3. Effect of trypsin preincubation (5 min) of spermatia on attachment to untreated trichogynes.

pretreatment	No. of trichogynes	No. of attached spermatia	spermatia /trichogynes
control	256	966	3.77
	271	894	3.30
0.05% (w/v) trypsin	311	483	1.55
	336	473	1.41
0.5% trypsin	257	15	0.06
	354	12	0.03

Table 4. Effect of degradation of vicinal-glycols of trichogyne coat on gamete attachment. (+; indicates present)

pretreatment of trichogyne		No. of	No. of	spermatia
oxidation	reduction	trichogynes	attached spermatia	/trichogynes
periodic acid	+	185	58	0.31
		76	24	0.32
hydrogen peroxide	+	126	570	4.52
		200	671	3.36
none (pH 4.0)	+	126	977	7.75
		239	387	2.78

Table 5. Time course of changes in the ratio of four nuclear stages[a] in all spermatia attached to the trichogyne.

time (min)	carpogonia			spermatia				
	total[b]	invaded[c]	karyogamy[d]	total[e]	state 1 (%)	state 2 (%)	state 3 (%)	state 4 (%)
30	170	0	0	1272	98	2	0	0
60	211	0	0	1329	54	38	7	1
120	165	7	4	1379	43	22	18	17
180	184	18	40	1267	37	12	19	33

[a] The four nuclear stages of spermatia are explained in results.

[b] All the carpogonia formed on the coverslip were counted.

[c] Carpogonia invaded by male nucleus, but karyogamy did not occur.

[d] Carpogonia where the carpogonium nucleus fused with male nucleus.

[e] All the spermatia that attached to the trichogynes were counted.

Table 6. Intra- and interspecific spermatium inoculation between Halosaccion yendoi from Akkeshi and Palmaria palmata from Muroran.

female	male	total number of trichogynes	number (%) of trichogynes of		
			state 1	state 2	state 3
Halosaccion	Halosaccion	102	30 (29)	11 (11)	61 (60)
		108	30 (28)	8 (7)	70 (65)
Palmaria	Palmaria	108	57 (53)	16 (15)	35 (32)
		103	57 (55)	16 (16)	30 (29)
Halosaccion	Palmaria	111	87 (78)	8 (7)	16 (15)
		118	80 (68)	6 (5)	32 (27)
Palmaria	Halosaccion	108	91 (84)	15 (14)	2 (2)
		106	80 (76)	16 (15)	10 (9)

PLATE 1

Figs. 1-9. Liberated spermatia of Palmaria palmata.

Fig. 1. Light micrograph using Nomarsky differential interferences-contrast optics. Living material. The cell is composed of vacuolar region (arrow) and nuclear region (arrowhead). Scale = 5 µm.

Fig. 2. Light micrograph of co-aggregated cells by agitation. Living material. Prepared in India ink/seawater. The cells (arrowhead) are covered with transparent coverings (arrow), which exclude carbon particles of India ink. Scale = 10 µm.

Fig. 3. DAPI-stained cells. a) Phase contrast and b) epifluorescence microscopy. Scale = 5 µm.

Figs. 4-9. TEM micrographs. Specimens were prepared by method A except for Figs. 7, 8.

Fig. 4. Median section showing a condensed spermatial nucleus, large vesicles (V), mitochondria (M), and small, dark-cored vesicles (arrowheads). Scale = 1 µm.

Figs. 5-9. Cell periphery. Scale in Fig. 5 (0.5 µm) applies also to Figs. 6-8.

Fig. 5. Peripheral tubules closely associated with peripheral ER (arrowheads).

Fig. 6. Close association (arrowheads) of peripheral tubules with dark-cored vesicles.

Figs. 7, 8. PATAg test of dark-cored vesicles.

Fig. 7. Section reacted with periodic acid. Vesicles are stained positively.

Fig. 8. Hydrogen peroxide control. An arrowhead indicates unstained vesicle.

Fig. 9. Dictyosome-like layered membranes (arrowhead) observed adjacent to a mitochondrion. Scale = 0.5 µm.

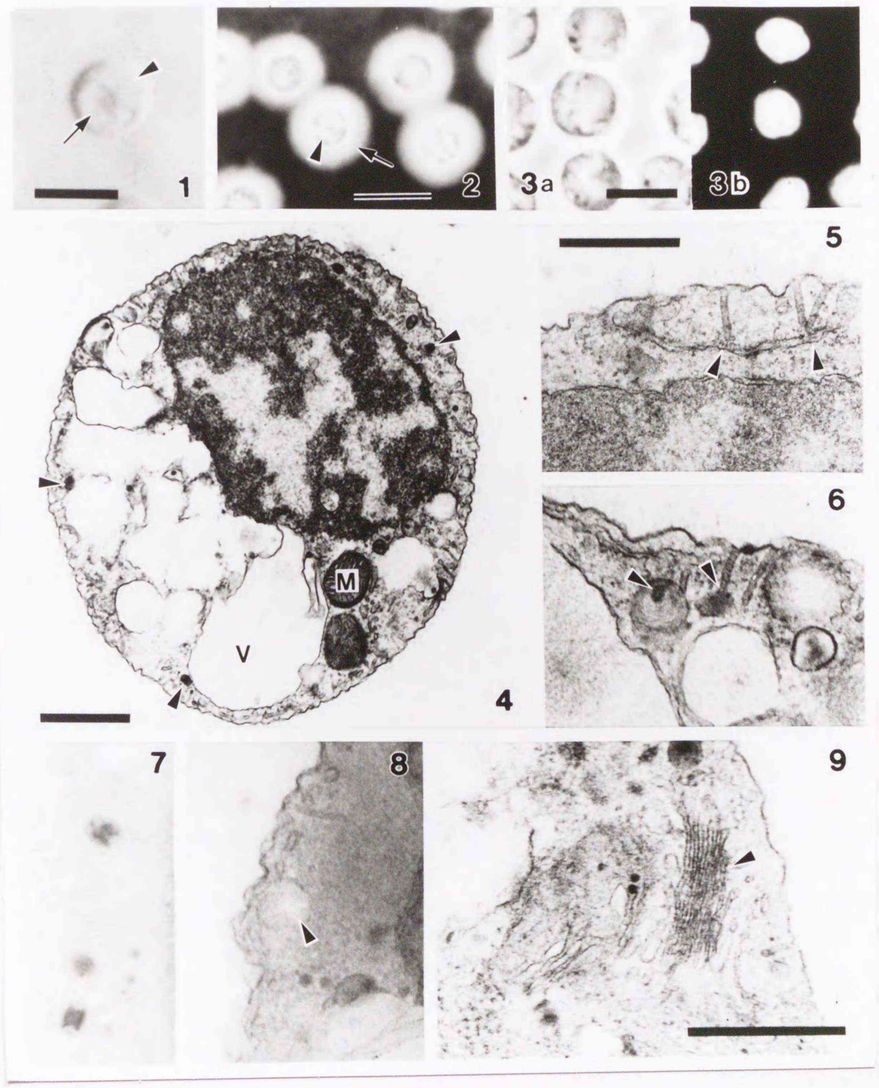

PLATE 2

Figs. 10-12. TEM micrographs of spermatia. Specimens were prepared by method A.

Fig. 10. Nucleus with a pair of PRs (arrowheads) above polar depressions of nuclear envelope. Scale = 1 µm.

Figs. 11a, b. Examples of a pair of PRs in another nucleus. Some extra- and intranuclear MTs (arrows) are assembled toward a PR. Scale = 0.5 µm.

Figs. 12a-d. Series of cross sections of polar depression of nuclear envelope. Scale = 0.2 µm. Fig. 12b is a tangential section of nuclear pores (arrowheads). Arrows indicate cross or oblique view of intra- (Fig. 12a) and extranuclear MTs (Figs. 12c, d).

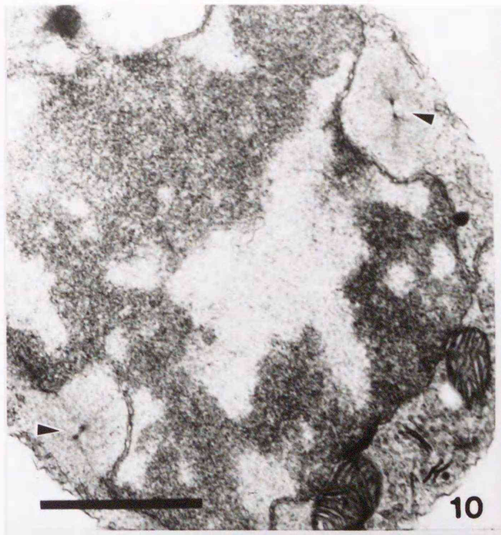

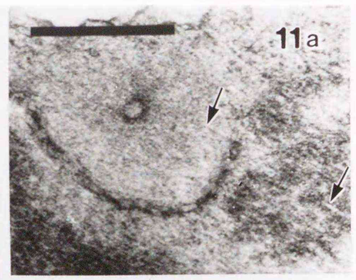

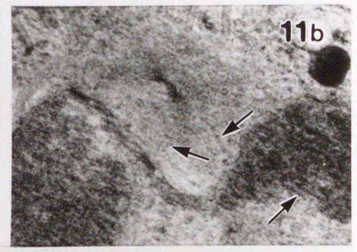

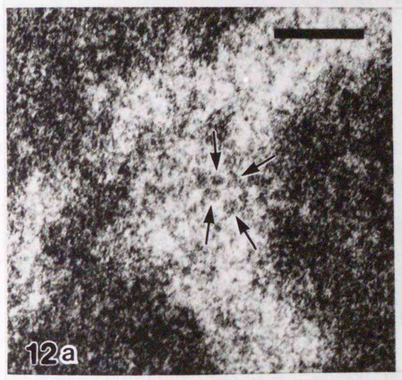

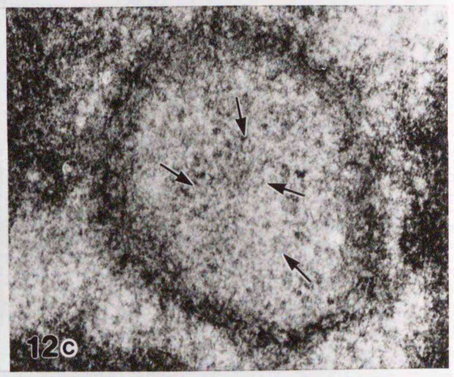

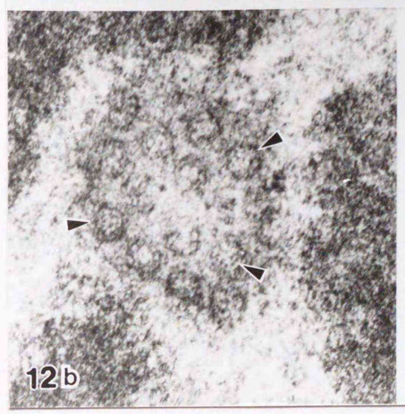

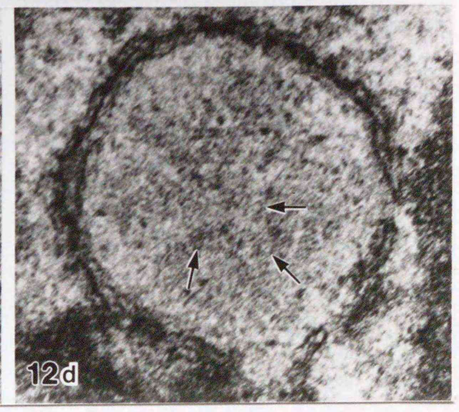

PLATE 3

Figs. 13-17. Spermatia prepared in India ink/seawater. Scale in Fig. 13 (10 µm) also applies to Figs. 14-17.

Figs. 13-15. Living materials. Scale in Fig. 12 (10 µm) also applies to Figs. 13-16.

Fig. 13. Untreated. Colorless coverings (arrow) uniformly observed around the cell (arrowhead).

Fig. 14. Treated with 1% Pronase E for 30 min. The spermatial covering (arrow) is thinner than that of untreated cells.

Fig. 15. Treated with 1% Pronase E for 120 min. The spermatial covering cannot be detected.

Figs. 16, 17. Spermatia fixed in 1% glutaraldehyde in ASW attached on coverslips coated with poly-L-lysin.

Fig. 16. In 90% ethanol after gradual dehydration. Shrunken spermatial coverings (arrows) outlined by sediment of carbon particles of India ink.

Fig. 17. In water after dehydration followed by gradual 're-hydration'. Spermatial coverings (arrows) have recovered in thickness.

Figs. 18-20. Transmission electron micrographs. Median section of spermatium. An asterisk indicates spermatial covering and an arrow indicates plasma membrane. Scale in Fig. 18 (0.5 µm) also applies to Figs. 19, 20. Prepared by method C.

Fig. 18. Untreated spermatium. Fibrous reticulated spermatial covering is observed around plasma membrane.

Fig. 19. Treated with 0.1% Pronase E for 90 min. The spermatial covering has thinned moderately.

Fig. 20. Treated with 1% Pronase E for 90 min. The spermatial covering is no longer detected.

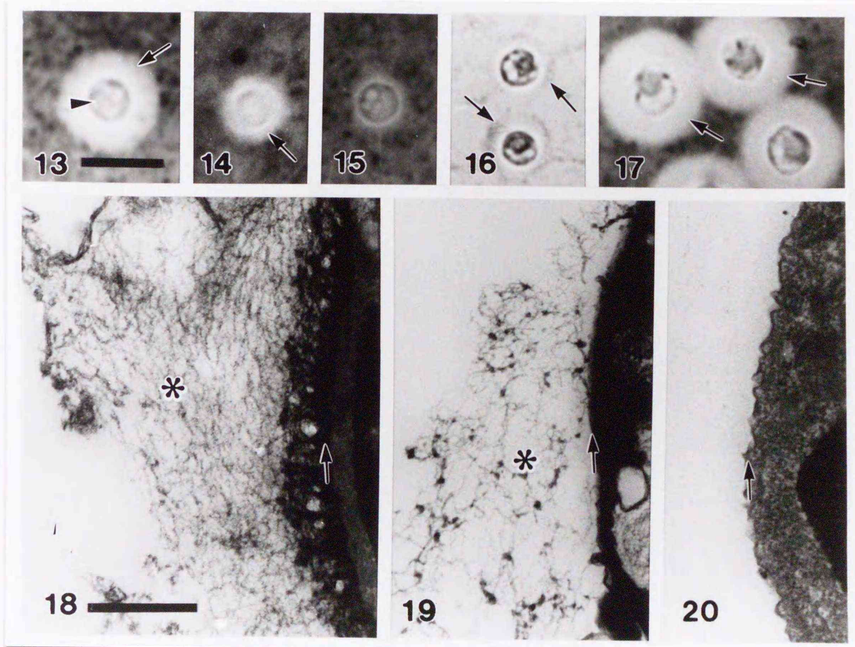

PLATE 4

Figs. 21, 22. Time course of thickness changes in non-fixed spermatial coverings during treatment with proteolytic enzymes. Data were expressed as % of control. Vertical lines indicate ± standard deviation. Controls were treated with ASW only.

Fig. 21. Treated with 1% (black square), 0.1% (white square), or 0.01% (black circle) Pronase E.

Fig. 22. Treated with 1% trypsin (white square), or 1% papain (black square).

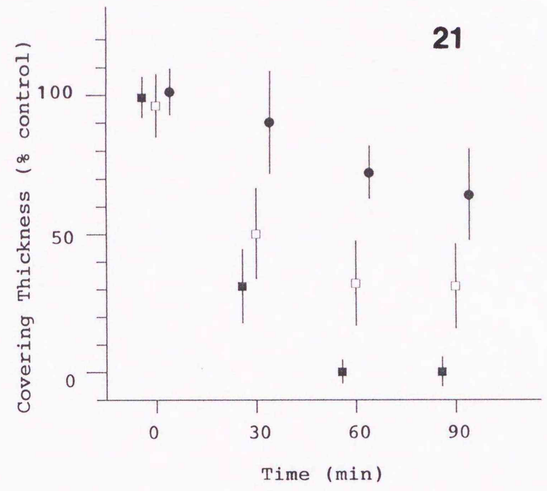

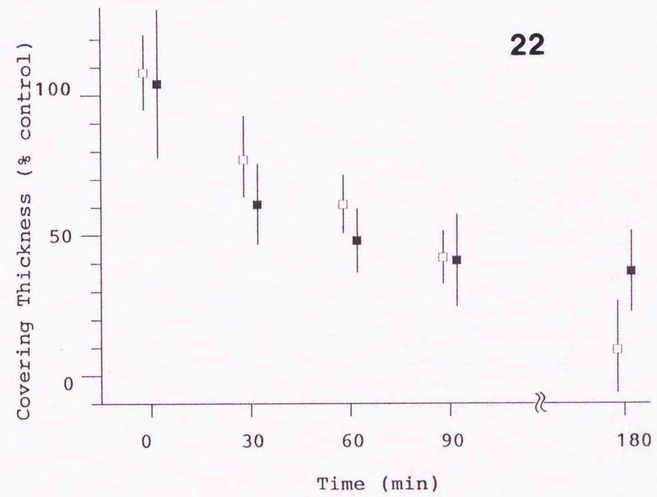

PLATE 5

Figs. 23-25. Time course of thickness changes in spermatial coverings during treatment with proteolytic enzymes. Data were expressed as % of control. Vertical lines indicate ± standard deviation. Controls were treated with ASW only.

Fig. 23. Non-fixed spermatial coverings. Treated with 0.5% trypsin (white square), or 0.5% trypsin along with 1mM PMSF (black square).

Fig. 24, 25. Glutaraldehyde-fixed spermatial coverings.

Fig. 24. Treated with 0.5% (white square), or 0.1% (black square) Pronase E.

Fig. 25. Treated with 0.5% (white square), or 0.1% (black square) trypsin.

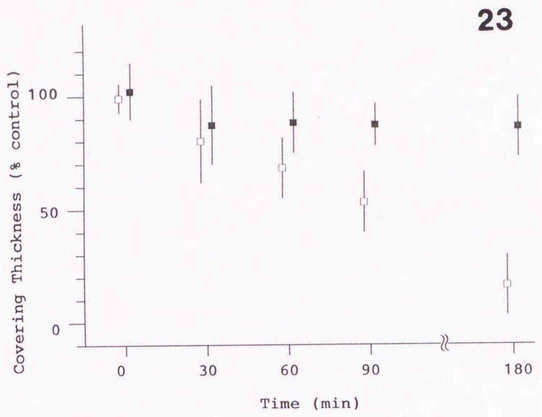

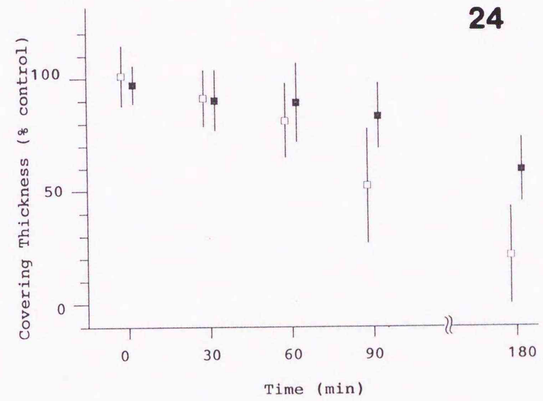

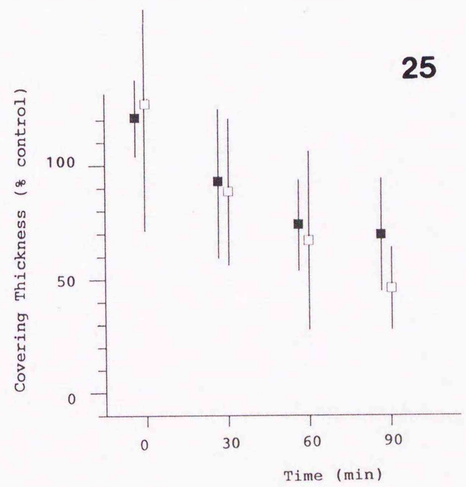

PLATE 6

Figs. 26-28. Transmission electron micrograph of development of spermatangia. Scales = 1 µm.

Figs. 26a, b. Serial sectioning of young spermatangium. Prepared by method A. Fig. 26a is the second section after the one shown in Fig. 26b. Electron-transparent vesicles (arrows) are secreted from whole surface of the spermatial cell inside the spermatangium cell wall.

Fig. 27. Young spermatangium. Method D. The secreted vesicles (arrows) contain fibrous, reticulate material.

Fig. 28. Spermatangium at a more advanced stage. Prepared by method D. Fibrous, reticulate material is observed in the gap (arrows) formed between the spermatial cell and spermatangium cell wall.

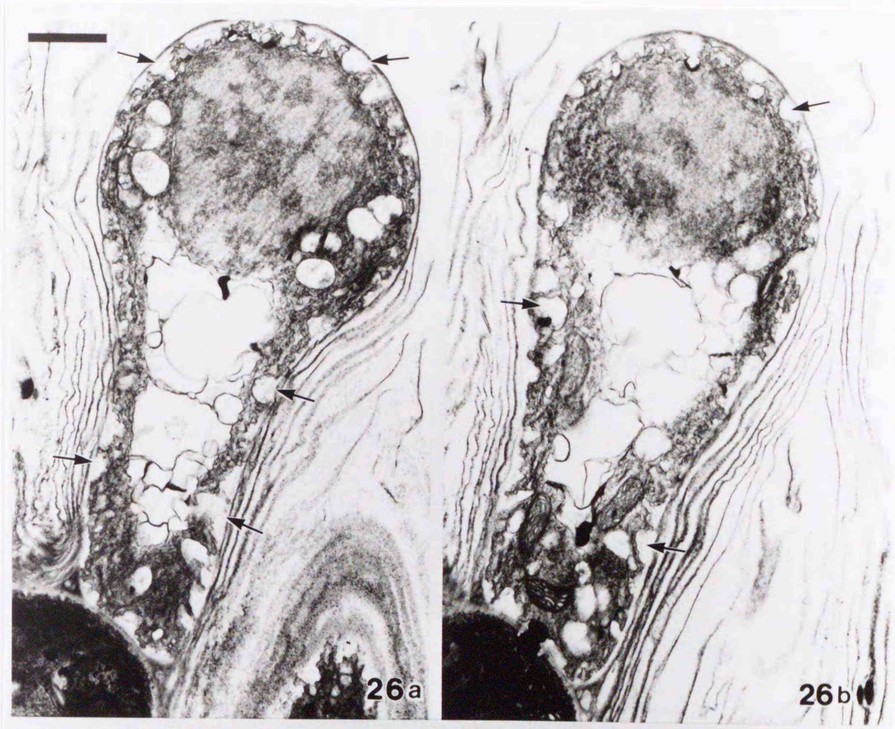

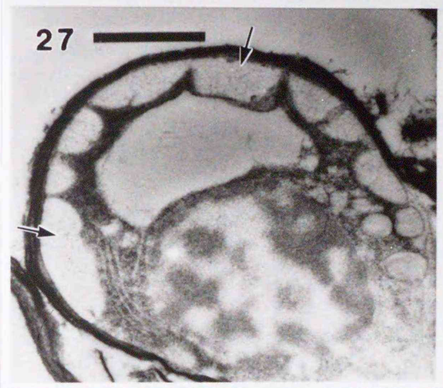

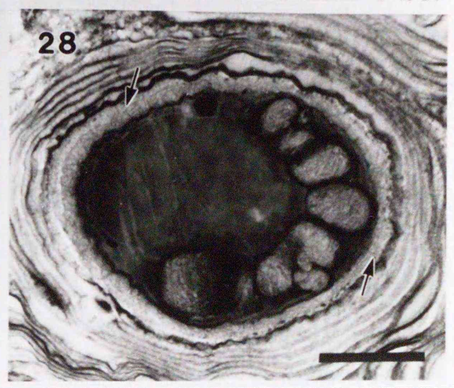

PLATE 7

Figs. 29-37. Transmission electron micrograph of trichogynes.

Figs. 29-31. Cross section of median portion. Scales = 1 µm.

Fig. 29. Prepared by method C. Fibrous trichogyne coat (arrowhead) is observed uniformly on the surface of the trichogyne cell wall (arrow).

Fig. 30. Method D. Radiating morphology of trichogyne coat further enhanced.

Fig. 31. Method E. Note the concentric arrangement of ERs (arrows) and a vacuole (V).

Figs. 32, 33. Longitudinal section of trichogyne apex. Scales = 1 µm.

Fig. 32. Method D. Fibrous trichogyne coat (arrow) is observed uniformly on the surface of the trichogyne apex.

Fig. 33. Method E. Small vesicles (arrows) are secreted within the apical thin cell wall, and densely arranged ERs are seen adjacent to the vesicles.

Fig. 34. Longitudinal section of median portion of trichogyne. Mitochondria (arrows) and a dictyosome (arrowhead) were seen. Prepared by method E.

Figs. 35-37. PATAg test on oblique section of trichogyne. Scale (1 µm) in Fig. 35 also applies to Figs. 36, 37.

Figs. 35, 36. Untreated trichogyne.

Fig. 35. Periodic acid oxidation. Trichogyne coat (arrow) is stained positively.

Fig. 36. Hydrogen peroxide control. Trichogyne coat (arrow) is stained negatively.

Fig. 37. Trichogyne after oxidation by periodic acid-sodium borohydride treatment. Periodic acid oxidation in PATAg test. Trichogyne coat (arrow) is very slightly PATAg-positive.

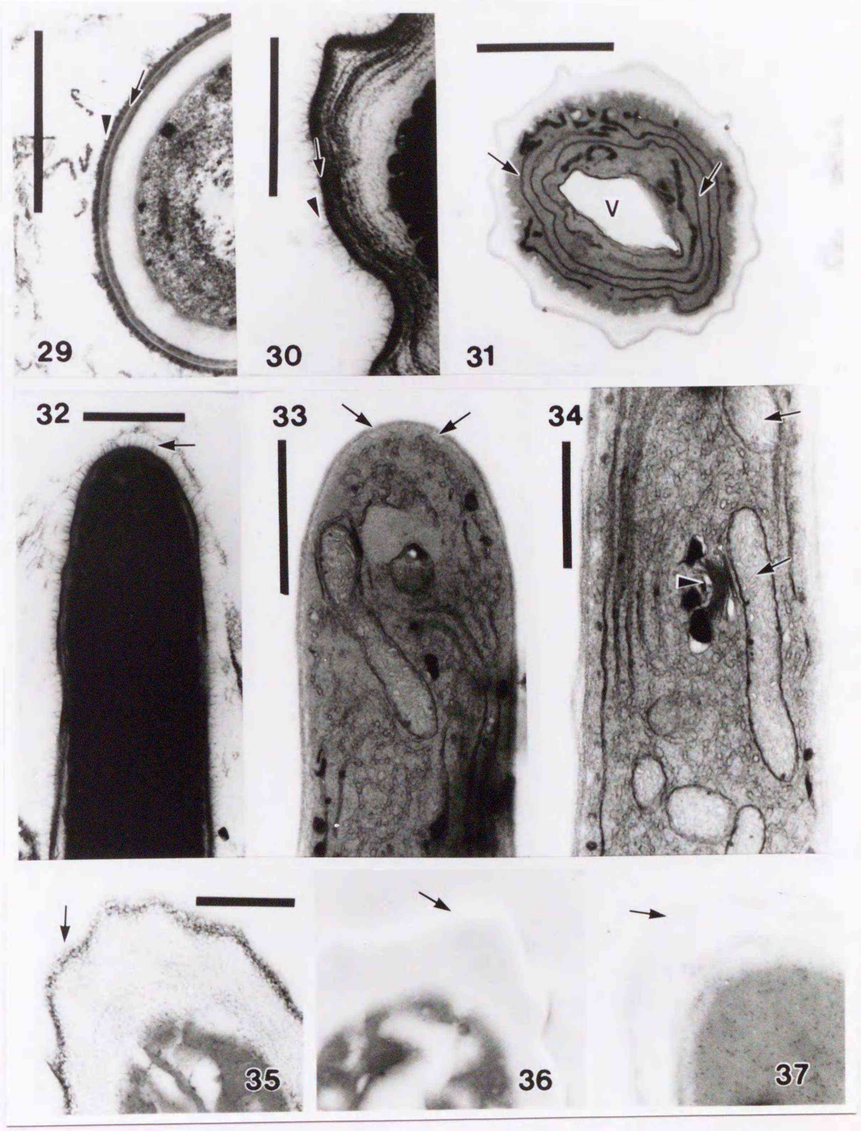

PLATE 8

Figs. 38-40. Attachment of spermatium to trichogyne.

Figs. 38a, b. Light microscopy. Examples of living material 5 min after spermatium inoculation. Prepared in India ink/seawater. An arrowhead indicates attachment of spermatial cell surface to trichogyne. Spermatial covering has been eliminated only at the site of attachment. Scale = 10 µm.

Figs. 39, 40. TEM micrographs of cross section of trichogyne (T) inoculated with spermatia. The cross section illustrated is where each spermatium was located in the closest position to the trichogyne in serial sectioning. Prepared by method C. Scale in Fig. 39 (0.5 µm) applies also to Fig. 40.

Fig. 39. Immediately after spermatium inoculation. Surface of spermatial covering (asterisk) is directly attached to the trichogyne coat (arrow).

Fig. 40. Five minutes after spermatium inoculation. The spermatial covering has been completely eliminated and spermatial plasma membrane (arrowhead) is tightly attached to trichogyne cell wall surface (arrow).

Figs. 41-44. Spermatial nuclear division. Light microscopy. DAPI-stained. a) Phase contrast. b) Epifluorescence. Scale in Fig. 41 (5 µm) applies also to Figs. 42-44.

Fig. 41. Further condensation of chromatin, or chromosomes, of spermatial nucleus observed 15 min after spermatium inoculation.

Fig. 42. Chromosomes aligned along the equatorial plate at 30 min.

Fig. 43. Segregation of chromosomes at 45 min.

Fig. 44. Binucleate spermatium at 60 min.

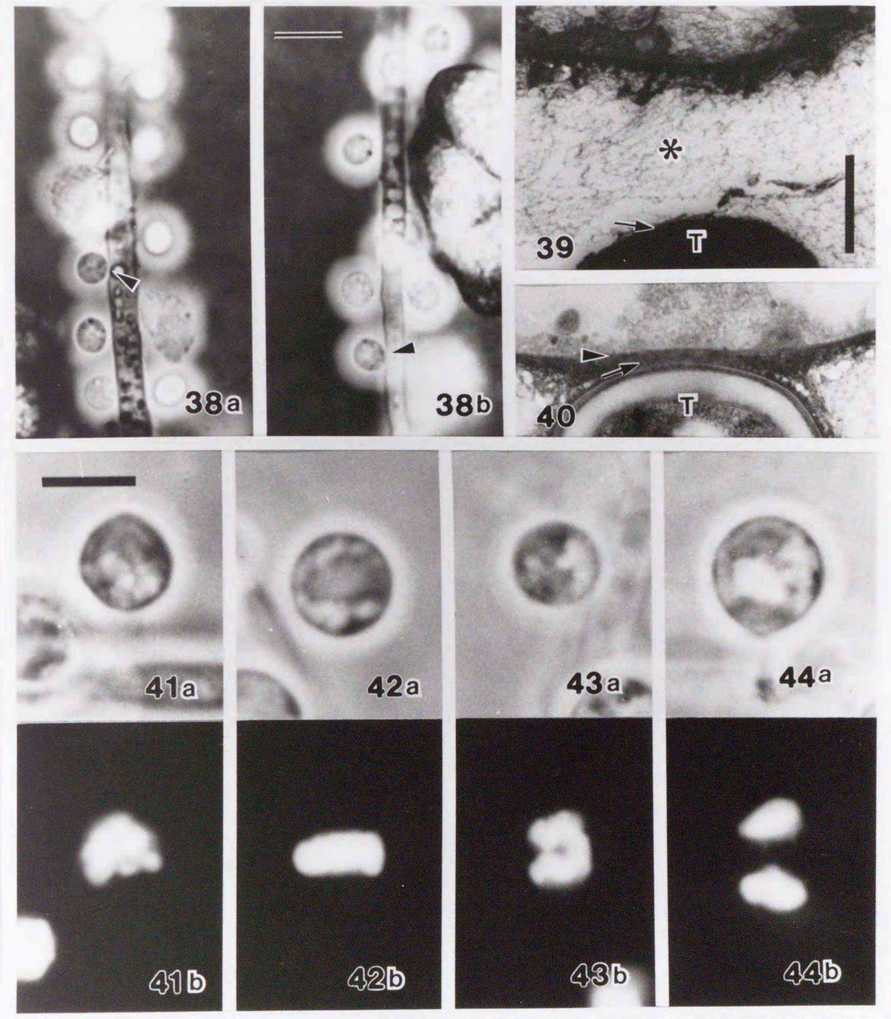

PLATE 9

Figs. 45-48. Ultrastructure of spermatial nuclear division. Prepared by method B.

Fig. 45. Prometaphase at 15 min. Arrowheads delimit nuclear envelope gap near the spindle polar region. Arrows indicate MTs. Scale = 1 µm.

Fig. 46. Early anaphase at 30 min. Arrows indicate upper and lower spindle polar regions. Fully condensed chromosomes with kinetochores (arrowheads) had moved slightly toward the polar regions. Scale = 1 µm.

Figs. 47a-c. Serial sectioning of the upper spindle polar region shown in Fig. 46. Scale = 0.2 µm. Fig. 47a is a magnification of Fig. 46. Arrows indicate MTs assembled toward the polar region. Continuity of nuclear envelopes along the region is unclear.

Figs. 48a, b. Examples of kinetochores observed in other metaphase or anaphase nuclei. Microtubule that appears to be associated with the kinetochore is indicated by an arrow. Scale = 0.2 µm.

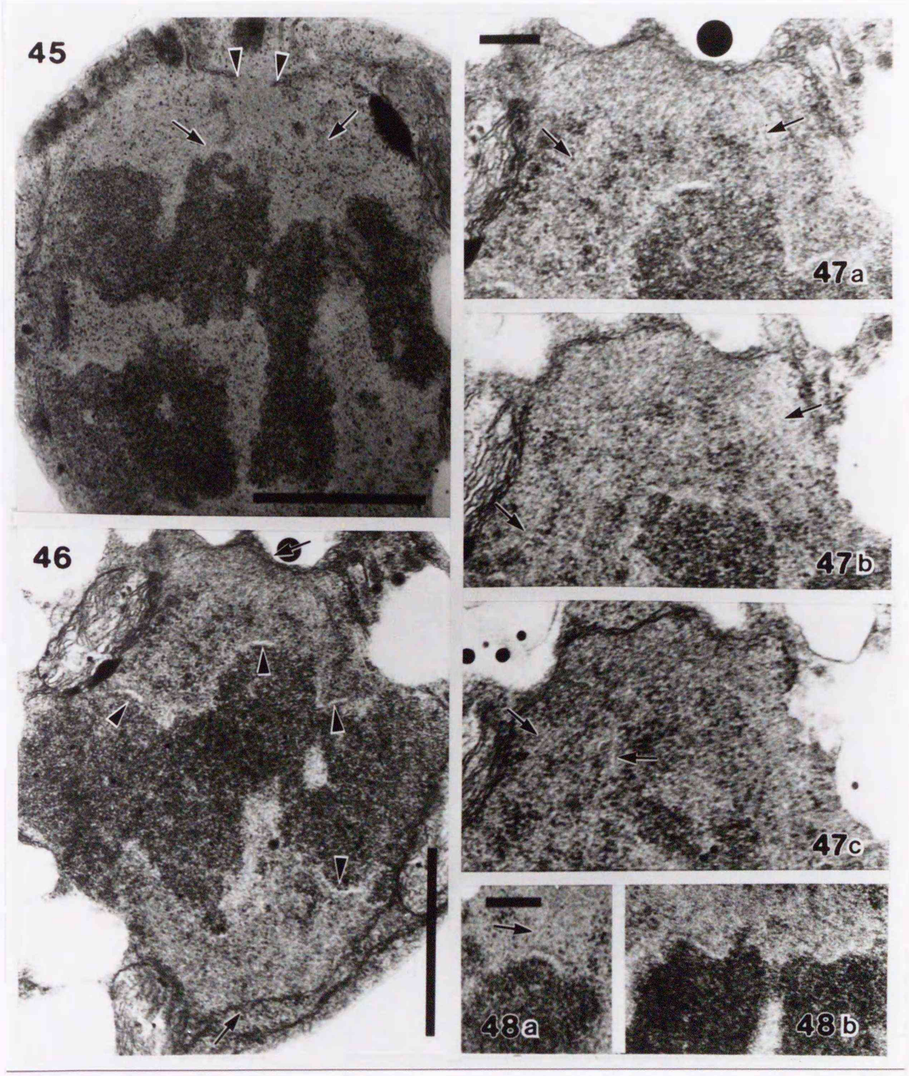

PLATE 10

Figs. 49a, b. Ultrastructure of an early telophase spermatial nucleus. Forty-five minutes after spermatium inoculation. Prepared by method B. Scale = 1 µm. Fig. 49a is the twenty-eighth section after the one shown in Fig. 49b. Nuclear envelopes (double arrowheads) are partially regenerated along segregated derivative nuclei (asterisk). Double arrows indicate remnant of nuclear envelope around interzonal midpiece. Kinetochores (arrowheads) remain facing toward large polar gap delimited by arrows.

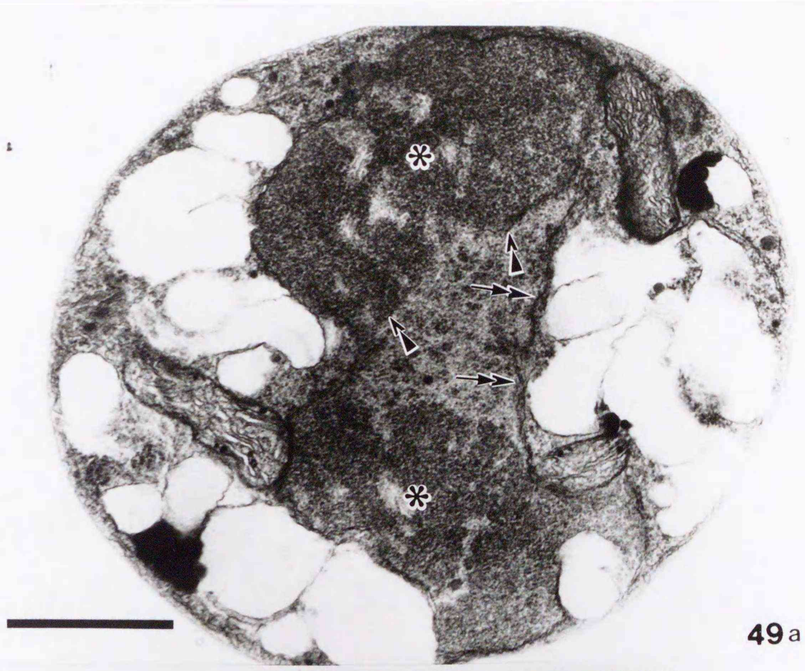

49a

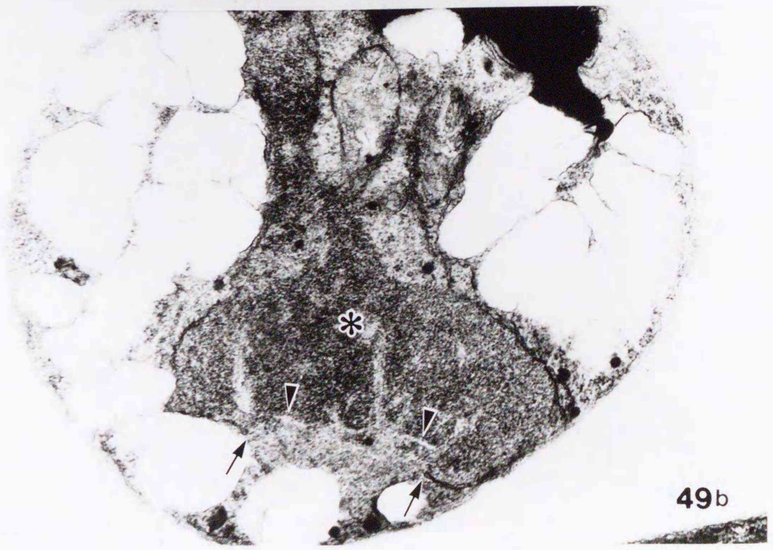

49b

PLATE 11

Figs. 50a, b. Ultrastructure of an early telophase spermatial nucleus. Forty-five minutes after spermatium inoculation. Prepared by method B. Scale = 1 µm. Fig. 50a is the seventh section after the one shown in Fig. 50b. Interzonal midpiece (double arrow) had been intensely constricted but nuclear envelopes of both derivative nuclei (asterisk) remain continuous with each other. Cytoplasmic components such as large electron-transparent vesicles and mitochondria have entered between the derivative nuclei. Nuclear envelopes (arrows) has partially regenerated along each polar gap. Kinetochores (arrowheads) remained facing toward the polar gap.

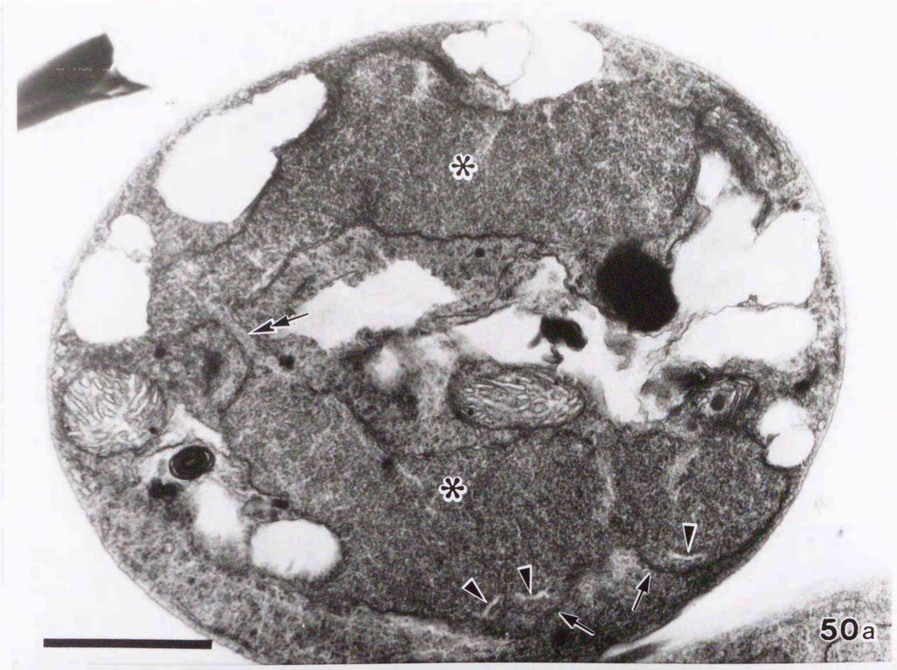

PLATE 12

Fig. 51. Ultrastructure of a spermatium that remained uninucleate 180 min after spermatium inoculation. Prepared by method A. Spermatial covering remains between spermatial plasma membrane (arrow) and trichogyne surface (T), and the PR (arrowhead) has not disappeared. Scale = 1 µm.

Figs. 52-55. Cell wall formation of spermatium.

Figs. 52, 53. Living material 60 min after spermatium inoculation. Stained with calcofluor. a) Phase contrast. b) Epifluorescence. Scale in Fig. 52 (5 µm) applies also to Fig. 53.

Fig. 52. Binucleate spermatium attached to trichogyne (T). Cell wall material is detected around the cell with two derivative nuclei (arrowheads).

Fig. 53. Uninucleate spermatium attached to trichogyne (T). Cell wall material is not detected.

Figs. 54, 55. PATAg test of cell wall of anaphase or telophase spermatium 45 min after spermatium inoculation. Scale in Fig. 54 (0.5 µm) also to Fig. 55.

Fig. 54. Section treated with periodic acid.

Fig. 55. Hydrogen peroxide control. PATAg-positive material (arrow) is detected around plasma membrane (arrowhead) in Fig. 54, but not in Fig. 55.

Figs. 56-59. Tetraspore germination of Palmaria palmata.

Figs. 56, 57. DAPI-stained. Epifluorescence. Scale in Fig. 56 (20 µm) also applies to Fig. 57.

Fig. 56. Sixty minutes after spore inoculation.

Fig. 57. Eighteen hours. Metaphase or anaphase nuclei are seen.

Figs. 58, 59. Calcofluor-stained. a) Bright field. b) Epifluorescence. Scale in Fig. 58 (20 µm) also applies to Fig. 59.

Fig. 58. Liberated tetraspore. No fluorescence is detected.

Fig. 59. Sixty minutes after inoculation. Calcofluor-positive material can be detected around the cell surface.

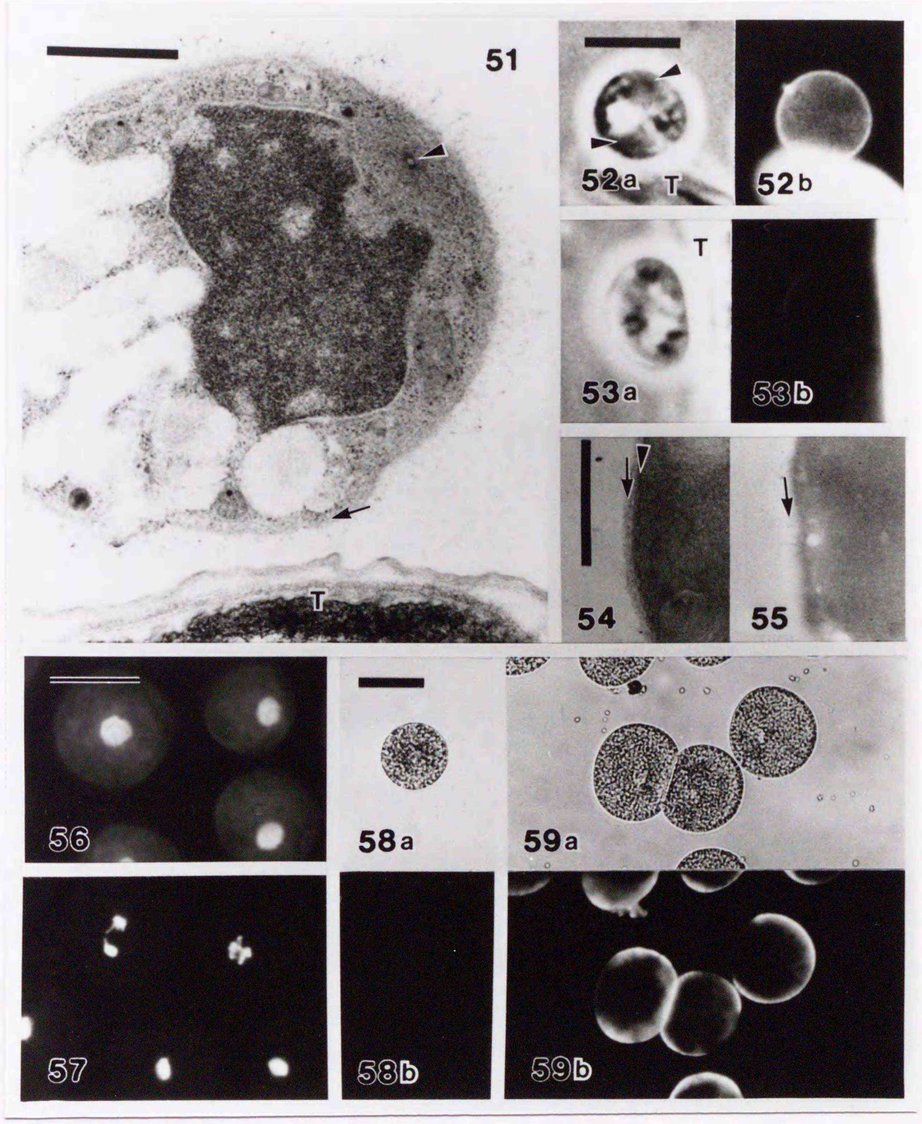

PLATE 13

Figs. 60-62. Gamete fusion. DAPI-stained. a) Brightfield. b, c) Epifluorescence. Scales = 5 µm.

Fig. 60. Invasion and migration of male nuclei to the trichogyne (T) 60 min after spermatium inoculation. One derivative nucleus (arrow) of the spermatium has invaded and another (double arrow) remains in the cell. An arrowhead indicates a migrating male nucleus from another fused spermatium.

Fig. 61. Nuclear fusion at 180 min. Carpogonial nucleus (arrowhead) with unstained nucleolus fuses with a condensed male nucleus (arrow). Double arrow indicates trichogyne of the carpogonium.

Fig. 62. Female germling 90 min after spermatium inoculation. Figs. a, b are in the same focal plane. Figs. b, c are epifluorescence in different focal planes. Two male nuclei (arrows) have invaded the carpogonial base of the germling. A carpogonial nucleus (arrowhead) fused with one of the male nuclei.

Figs. 63-65. Ultrastructure of cytoplasmic fusion process between binucleate spermatium (one of two male nuclei designated an asterisk) and trichogyne cytoplasm (T). Scale in Fig. 63 (0.5 µm) applies also to Figs. 64, 65.

Figs. 63, 64. Sixty minutes after spermatium inoculation. Prepared by method B.

Fig. 63. Binucleate spermatium tightly attached to trichogyne cell wall surface. An arrow indicates cell wall surface of the trichogyne and an arrowhead indicates the plasma membrane of the spermatium.

Fig. 64. Invasion and expansion of spermatial cytoplasm (arrowheads) into trichogyne cell wall. Fig. 65. Cytoplasmic fusion observed at 120 min. Method A.

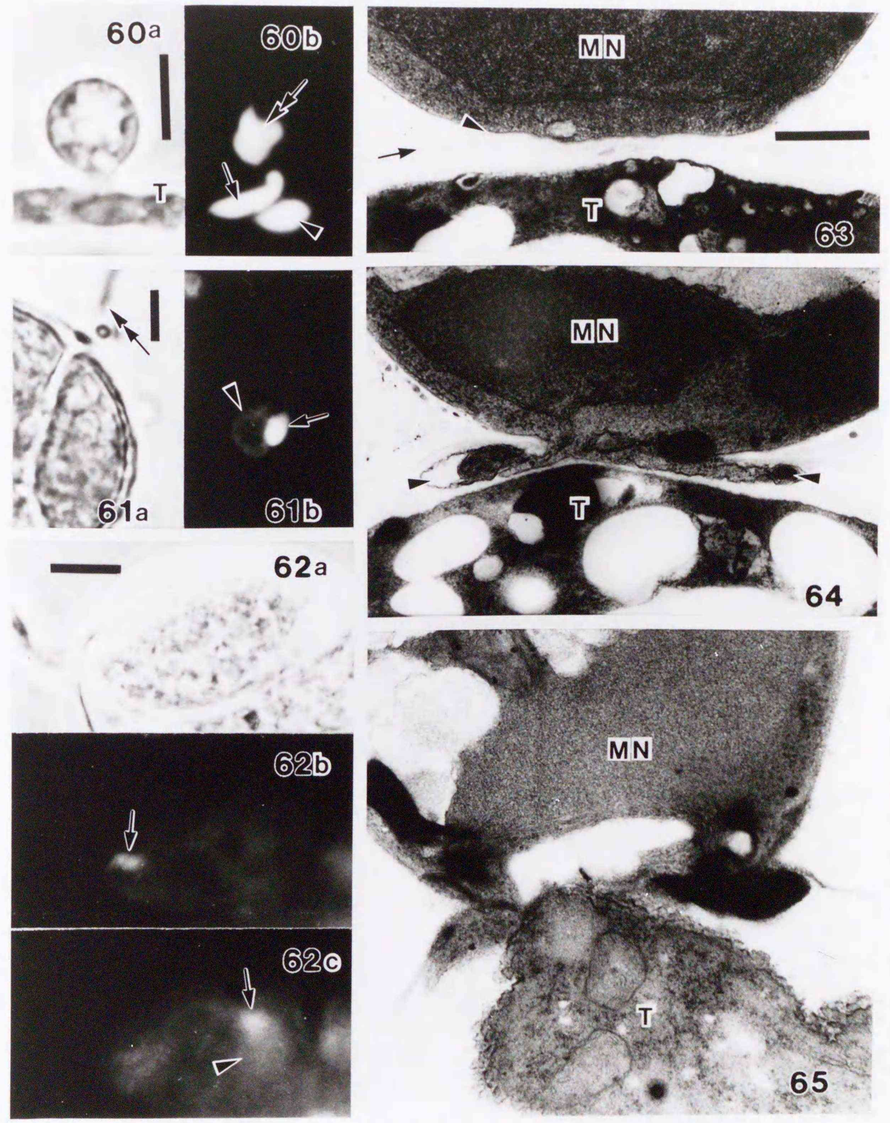

PLATE 14

Fig. 66. Spermatial cell (asterisk) and opening between fused spermatial cytoplasm and trichogyne cytoplasm after invasion of two male nuclei at 180 min after spermatium inoculation. Method A. Mitochondria, large vesicles and electron-dense body were left in the cytoplasm of the spermatium. Mitochondria and membraneous structures were observed within the opening. Scale = 1 µm.

Figs. 67-69. Ultrastructure of migrating male nucleus (asterisk) at 180 min.

Fig. 67. Male nucleus migrating in the trichogyne. Method A. Scales = 2 µm.

Fig. 68. Male nucleus migrating in the trichogyne. Method B. Scales = 1 µm.

Fig. 69. Serial sectioning of male nucleus in carpogonial base associated with MTs (arrows). An arrowhead indicates MT-filled nuclear groove. Scales = 1 µm.

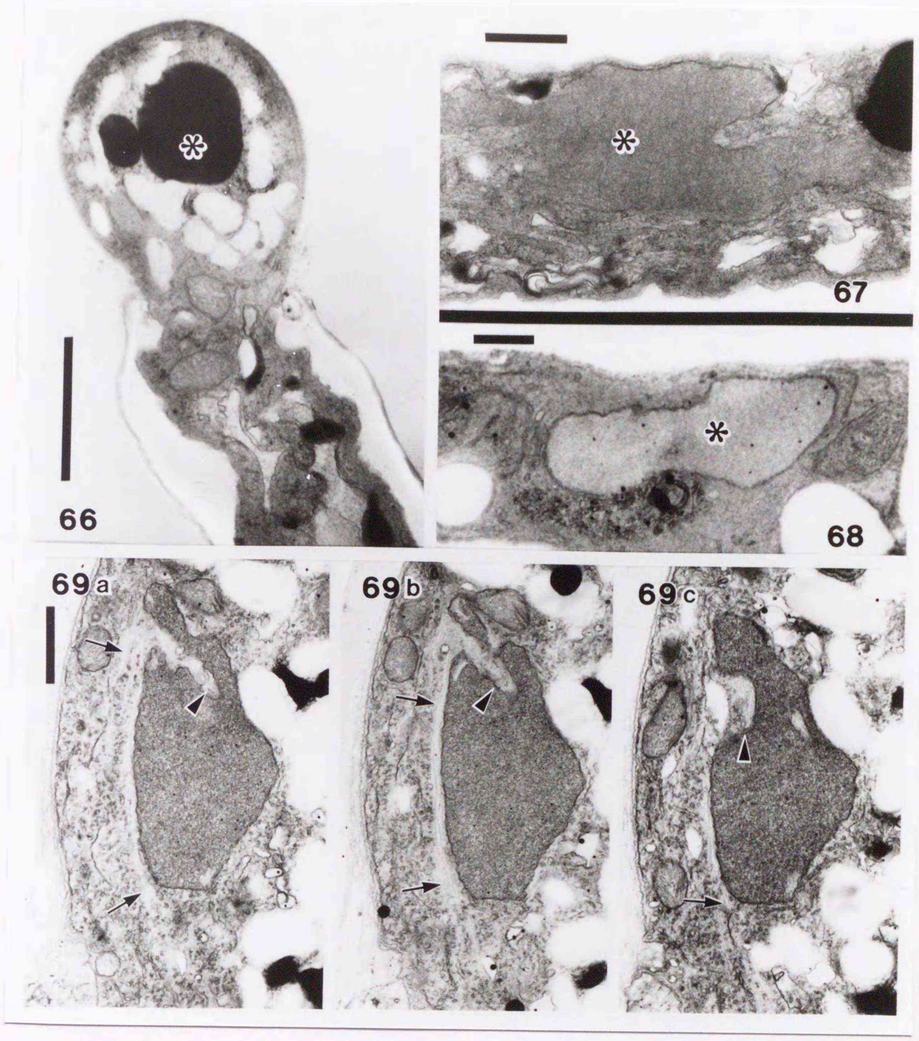

PLATE 15

Figs. 70-72. Ultrastructure of female gametophyte.

Fig. 70. Serial oblique sectioning of the basal portion of trichogyne (T). Arrows indicate the electron-transparent outline of inner primary cell wall of female germling. b) is the second section from a). Scale = 2 µm.

Figs. 71, 72. Ultrastructure of carpogonial nucleus that co-existed with the male nucleus of Fig. 69 in the same carpogonial base. Method B.

Fig. 71. Median section. Scale = 1 µm.

Fig. 72. Tangential section showing nuclear pores (arrow). Scale = 0.2 µm.